Cancer Cell

Article

Daily glucocorticoids promote glioblastoma growth and circadian synchrony to the host

Graphical abstract

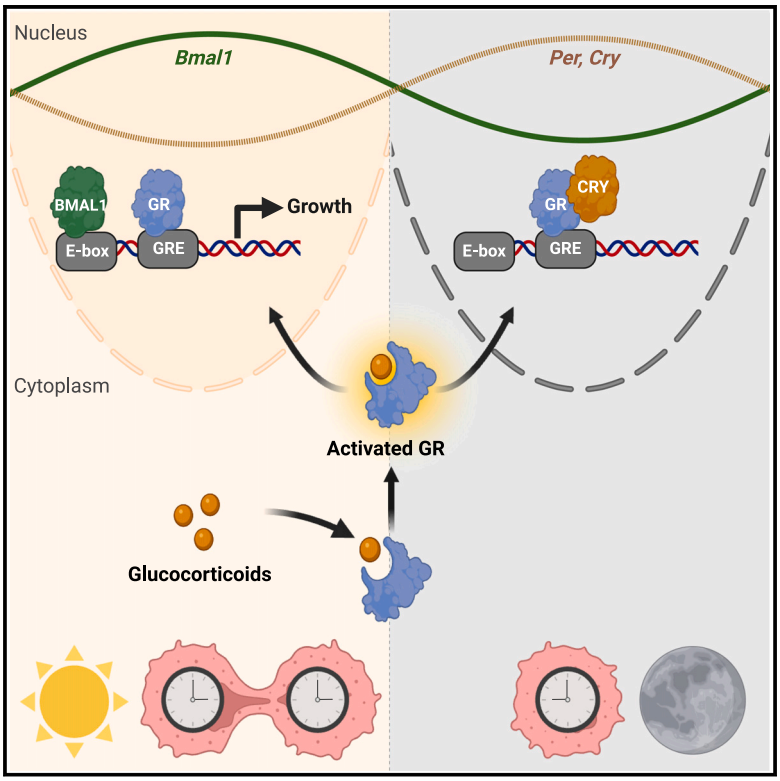

Authors

Maria F. Gonzalez-Aponte, Anna R. Damato, Tatiana Simon, ..., Jingqin Luo, Joshua B. Rubin, Erik D. Herzog

Correspondence

herzog@wustl.edu

In brief

Gonzalez-Aponte et al. identify daily glucocorticoid receptor signaling as an intrinsic driver of glioblastoma (GBM) progression and a synchronizer of tumor clock gene expression to the host. This work provides an intrinsic circadian driver, and therapeutic target, to slow GBM growth, and offers considerations for glucocorticoid use in the clinic.

Highlights

- Glucocorticoids promote glioblastoma (GBM) growth in a time-of-day dependent manner
- Loss of daily glucocorticoid signaling reduces GBM growth and disease progression
- Mouse and human GBM cells have intrinsic daily rhythms that synchronize to the host
- Glucocorticoids synchronize daily clock gene expression in GBM

Gonzalez-Aponte et al., 2025, Cancer Cell *43*, 1–17
January 13, 2025
https://doi.org/10.1016/j.ccell.2024.11.012

CellPress

Cancer Cell

CellPress
OPEN ACCESS

Article

Daily glucocorticoids promote glioblastoma growth and circadian synchrony to the host

Maria F. Gonzalez-Aponte,[1] Anna R. Damato,[1] Tatiana Simon,[1] Nigina Aripova,[1] Fabrizio Darby,[1] Myung Sik Jeon,[2,3] Jingqin Luo,[2,3] Joshua B. Rubin,[4,5] and Erik D. Herzog[1,6,*]

[1]Department of Biology, Division of Biology and Biomedical Sciences, Washington University in St. Louis, St. Louis, MO 63130, USA
[2]Department of Surgery, Division of Public Health Sciences, Washington University School of Medicine, St. Louis, MO 63110, USA
[3]Siteman Cancer Center Biostatistics Shared Resource, Division of Public Health Sciences, Department of Surgery, Washington University School of Medicine, St. Louis, MO 63110, USA
[4]Department of Pediatrics, St. Louis Children's Hospital, Washington University School of Medicine, St. Louis, MO 63110, USA
[5]Department of Neuroscience, Washington University School of Medicine, St. Louis, MO 63110, USA
[6]Lead contact
*Correspondence: herzog@wustl.edu
https://doi.org/10.1016/j.ccell.2024.11.012

SUMMARY

Glioblastoma (GBM) is the most common primary malignant brain tumor in adults with a poor prognosis despite aggressive therapy. Here, we hypothesized that daily host signaling regulates tumor growth and synchronizes circadian rhythms in GBM. We find daily glucocorticoids promote or suppress GBM growth through glucocorticoid receptor (GR) signaling depending on time of day and the clock genes, *Bmal1* and *Cry*. Blocking circadian signals, like vasoactive intestinal peptide or glucocorticoids, dramatically slows GBM growth and disease progression. Analysis of human GBM samples from The Cancer Genome Atlas (TCGA) shows that high GR expression significantly increases hazard of mortality. Finally, mouse and human GBM models have intrinsic circadian rhythms in clock gene expression *in vitro* and *in vivo* that entrain to the host through glucocorticoid signaling, regardless of tumor type or host immune status. We conclude that GBM entrains to the circadian circuit of the brain, modulating its growth through clock-controlled cues, like glucocorticoids.

INTRODUCTION

Glioblastoma (GBM) is the most common malignant and deadly brain tumor in adults.[1,2] Despite an aggressive treatment paradigm that includes maximal safe surgical resection, radiation plus concomitant and adjuvant chemotherapy with temozolomide (TMZ), and tumor-treating fields, median survival time post-treatment is 15 months, and 5-year survival is less than 5% after diagnosis.[1,3,4] These devastating trends emphasize the importance of identifying new therapeutic targets and approaches that can improve outcomes for GBM patients. One recent approach shown to maximize response to chemotherapy and extend survival in cellular and animal models of GBM, as well as in human patients, is administering TMZ in accordance with time of day.[5–8] A recent retrospective clinical study finds that taking TMZ in the morning compared to the evening is associated with a 6-month increase in median survival.[6] We recently demonstrate that circadian regulation in expression of the DNA repair enzyme, O6-methylguanine-DNA methyltransferase (MGMT), underlies daily rhythms in TMZ sensitivity in cellular and animal models of GBM.[8] These findings suggest that circadian rhythms in GBM may regulate tumor biology and response to therapies.

In addition to therapies that aim to reduce tumor growth, GBM patients are currently treated with corticosteroids around the time of surgery and radiation, and often at the time of terminal progression, to reduce GBM-induced cerebral edema.[9–11] Dexamethasone (DEX) is the drug of choice among synthetic glucocorticoids (GCs, cortisol in humans and corticosterone in rodents) due to its ability to decrease the permeability of the blood brain barrier,[9,12–14] high specificity for the glucocorticoid receptor (GR), long half-life, and high potency.[10] However, glucocorticoid action has been variably implicated in tumor progression.[11] Several studies show tumor suppressive effects of DEX in patients and in various GBM models *in vitro* and *in vivo*.[15–19] Others demonstrate that DEX promotes GBM cell proliferation and a glioma stem cell-like phenotype, decreases host survival, and induces resistance to chemotherapy with TMZ.[11,20–25] None of these studies have controlled for the possibility of glucocorticoid action varying with time of day or whether daily activation of the glucocorticoid signaling pathway drives GBM progression. Because glucocorticoid levels increase dramatically each day prior to waking[26–30] under circadian control,[31] we hypothesized that daily glucocorticoid signaling regulates tumor progression dependent on circadian time in GBM.

Please cite this article in press as: Gonzalez-Aponte et al., Daily glucocorticoids promote glioblastoma growth and circadian synchrony to the host, Cancer Cell (2024), https://doi.org/10.1016/j.ccell.2024.11.012

Unlike other cancers where circadian rhythms tend to be disrupted, well-studied murine, human, and primary GBM models have reliable circadian rhythms in clock gene expression and sensitivity to therapies.[5,8,32,33] This leads to the hypothesis that GBM tumors act as peripheral circadian pacemakers that synchronize (entrain) their daily rhythms to the host to regulate tumorigenic processes. To maintain synchronized circadian rhythms in physiology and behavior, all vertebrates depend on a central circadian pacemaker in the suprachiasmatic nucleus (SCN) of the brain that entrains its daily rhythms in clock gene expression through light and neuropeptides, such as pituitary adenylate cyclase-activating peptide (PACAP) and vasoactive intestinal peptide (VIP).[34–40] The SCN, in turn, regulates daily rhythms in the rest of the body through signals, including body temperature,[41,42] glucocorticoids,[43,44] and insulin/insulin-like growth factor (IGF) in combination with glucose.[45–47] Among these, glucocorticoids are one of the highest amplitude circadian outputs, and suffice to synchronize circadian clocks in tissues including brain, liver, kidney, and heart.[43] Here we test the hypothesis that daily glucocorticoid signaling synchronizes circadian rhythms in GBM to the host. Altogether, we find that blocking the daily peak of glucocorticoid signaling desynchronizes circadian rhythms in GBM from the host and dramatically slows disease progression in tumor-bearing mice.

RESULTS

Glucocorticoids promote GBM growth through glucocorticoid receptor signaling dependent on circadian time

Glucocorticoids like DEX are reported to either promote or suppress GBM tumor growth.[11,15–25] This variable response could be due to direct effects on glucocorticoid receptor (GR) signaling in different contexts, such as the time of day when DEX was delivered, or through GR-independent pathways. We hypothesized that known circadian variation in daily glucocorticoid secretion and clock-controlled GR signaling might underlie the variability in tumor growth effects. We used the well-characterized human LN229 and murine GL261 GBM cell lines, which have been previously found to have reliable circadian rhythms in clock gene expression and response to TMZ chemotherapy.[8] We transduced LN229 and GL261 GBM cultures with luciferase reporters driven by the promoters of the clock genes *Bmal1* or *Per2* (Figure 1A). Real-time *in vitro* bioluminescence recordings showed that GBM cells have intrinsic daily rhythms in *Bmal1* (B1L, green) and *Per2* (P2L, yellow) expression (Figures 1B, 1C, and S1A–S1C), with *Bmal1* consistently peaking approximately 10 h before peak *Per2* expression, and a circadian period ranging from 23 h to 31 h (Figures S1A–S1C). We next treated LN229-P2L and GL261-P2L cultures with 100 nM of the synthetic glucocorticoid DEX or vehicle (0.001% ethanol) at either the daily peak or trough of *Per2* expression. We found that DEX promoted about a 3-fold increase in GBM growth when delivered around trough of *Per2* but suppressed growth by about 3-fold at the peak, in both cell lines (Figures 1D and 1E). To test whether this time-dependent effect of DEX on tumor growth depended on GBM-intrinsic GR signaling, we reduced GR expression in LN229-P2L and GL261-P2L GBM cells using viral-mediated knock-down (hereafter, GR KD; Figures S2A–S2D). Knocking down GR by approximately 62% or 87% in LN229 and GL261 cells, respectively, did not affect intrinsic cell growth or daily *Per2* expression *in vitro* (Figures S2E–S2H), but eliminated the time-dependent DEX-induced GBM growth *in vitro* (Figures 1F and 1G). To assess whether GBM cells exhibit daily rhythms in GR expression, we collected mRNA from LN229 cells every 4 h over 48 h and performed qPCR to measure *Nr3c1* (GR) and *Bmal1* gene expression. We found daily rhythms in *Bmal1* and GR expression in LN229 cells, with transcription of both genes peaking at circadian time (CT) 12 (Figures S2I and S2J). These results are consistent with previous measurements of clock gene transcription (i.e., *Bmal1*:luc reporter) and indicate circadian regulation of GR expression. Altogether, these results suggest that glucocorticoids, like DEX, can regulate GBM growth directly through rhythmic GR signaling as a function of circadian time.

To evaluate *in vivo* glucocorticoid effects as a function of time of day, we first characterized daily clock gene expression in orthotopic GBM xenografts. We implanted human LN229 cells into immunocompromised nude mice or murine GL261 cells into immunocompetent C57Bl/6NJ mice housed in a light/dark cycle (LD, where lights on is defined as zeitgeber time (ZT) 0 and lights off as ZT12). GBM cells expressed either the *Bmal1*- or *Per2*-luciferase reporter. Approximately 10 days after implantation into the basal ganglia, we imaged *in vivo* bioluminescence every 4 h over 36 h from anesthetized mice (Figure 2A). We found reliable daily rhythms in tumor clock gene expression *in vivo*, with *Bmal1* peaking in the early morning (ZT4) and *Per2* peaking at night (ZT18; Figures 2B–2E). Additional recordings of *Bmal1* and *Per2* expression from GL261 or LN229 xenografts in freely moving mice also showed anti-phase circadian rhythms in clock gene expression over 72 h in constant darkness, with *Bmal1* peaking during the subjective day and *Per2* peaking at night (Figures S3A–S3E).

Because GBM tumors are highly heterogeneous, we tested whether circadian rhythms in clock gene expression differ among additional human and mouse GBM models. We found similar anti-phase daily rhythms in *Bmal1* and *Per2* expression recorded *in vitro* and from *in vivo* orthotopic xenografts of a murine GBM model ($NF1^{-/-}$ DNp53) and a primary human GBM isolate (B165) (Figures S4A–S4H). Consistent with our findings with GL261 and LN229, *Bmal1* peaked during the day and *Per2* peaked at night in $NF1^{-/-}$ DNp53 and B165 GBM tumors *in vivo* (Figures S4E–S4H). To assess whether daily rhythms in clock gene expression change with disease progression *in vivo*, we repeatedly imaged GL261-P2L xenografts at 11 and 18 days post-implant. We found that, as the tumors grew and mice lost body weight from 11 to 18 days post-implant (Figure S5A), *Per2* reliably peaked during the night (ZT16; Figures S5B–S5E). Together, these data demonstrate that clock gene expression is conserved across diverse GBM tumors *in vitro* and *in vivo*, and that these daily cycles of clock gene expression synchronize to their host regardless of host immune status and over the course of disease progression.

To test if glucocorticoids act directly to promote GBM proliferation as a function of circadian time *in vivo*, we implanted mice with either human LN229, with or without GR, or murine GL261 cells, and tracked tumor size by *in vivo* bioluminescence imaging. Once tumor growth was established at 11 days

Please cite this article in press as: Gonzalez-Aponte et al., Daily glucocorticoids promote glioblastoma growth and circadian synchrony to the host, Cancer Cell (2024), https://doi.org/10.1016/j.ccell.2024.11.012

CellPress
OPEN ACCESS

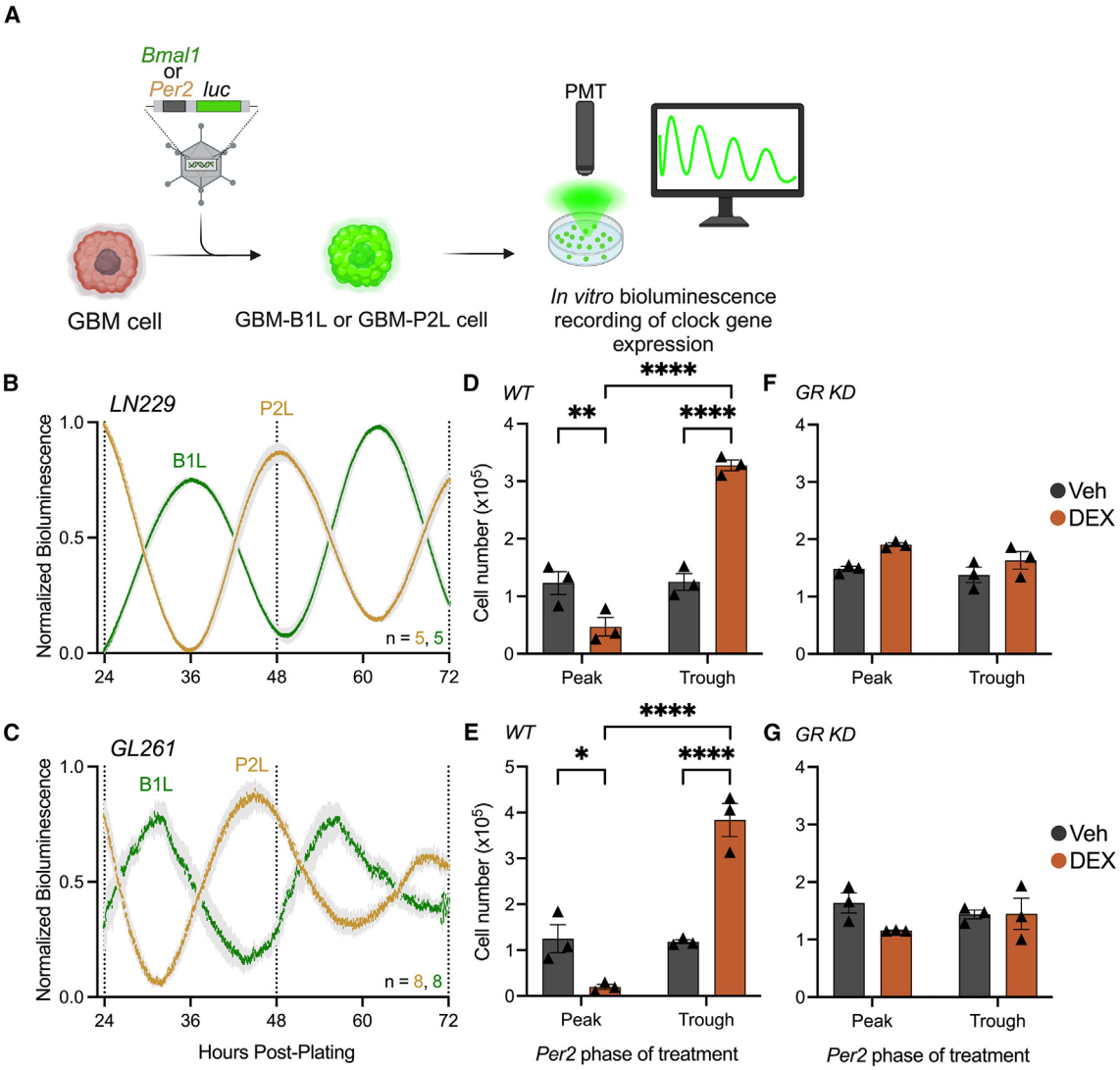

Figure 1. Dexamethasone promotes GBM growth through glucocorticoid receptor signaling dependent on circadian time of treatment *in vitro*

(A) Schematic of cell transduction with reporters of clock gene (*Period2*, *Per2*, or *Bmal1*) expression.

(B and C) Human LN229 (B) and murine GL261 (C) GBM cell lines transduced with a *Per2*- or *Bmal1-driven* luciferase reporter (*Per2*:luc [P2L] and *Bmal1*:luc [B1L], respectively) show circadian rhythms in clock gene expression *in vitro* (mean ± SEM, *n* reported in figure, all recordings had cosine fits with correlation coefficients, CC > 0.9).

(D and E) Acute treatment of LN229 (D) and GL261 (E) GBM WT cells with 100 nM DEX *in vitro* suppressed cell proliferation about 3-fold when added at the peak of daily *Per2* expression, and increased growth about 3-fold when administered at the trough (mean ± SEM, *n* = 3 per group, two-way ANOVA with Šídák's multiple comparisons test, $*p < 0.05$, $**p < 0.01$, $****p < 0.0001$).

(F and G) LN229 (F) and GL261 (G) cells lacking the glucocorticoid receptor (GR KD) did not proliferate in response to DEX treatment at either the daily peak or trough of *Per2* expression *in vitro* (mean ± SEM, *n* = 3 per group, two-way ANOVA with Šídák's multiple comparisons test, ns $p > 0.05$). See also Figures S1 and S2.

post-implant, we delivered 0.5 mg/kg DEX or vehicle (water) by oral gavage for 6 consecutive days at either 4-h (ZT4) or 12-h (ZT12) after daily light onset (corresponding to the trough or peak of tumor *Per2* expression, respectively). To control for the effects of mouse handling, we treated all mice with vehicle by oral gavage at the times when they did not receive DEX (Figure 2F). We found that LN229 and GL261 tumor size significantly increased by 2- and 5-fold, respectively, in mice receiving DEX in the morning, compared to evening and vehicle treatments (Figures 2G and 2H). No significant differences between morning and evening DEX treatment were found in mice bearing LN229 GR knockdown (KD) tumors (Figure 2G). Mice bearing LN229 and GL261 WT tumors treated with DEX in the morning lost significantly more weight than those treated in the evening or with vehicle, or those bearing an LN229 GR KD tumor, indicating greater disease progression (Figures 2I and 2J). As an additional

Please cite this article in press as: Gonzalez-Aponte et al., Daily glucocorticoids promote glioblastoma growth and circadian synchrony to the host, Cancer Cell (2024), https://doi.org/10.1016/j.ccell.2024.11.012

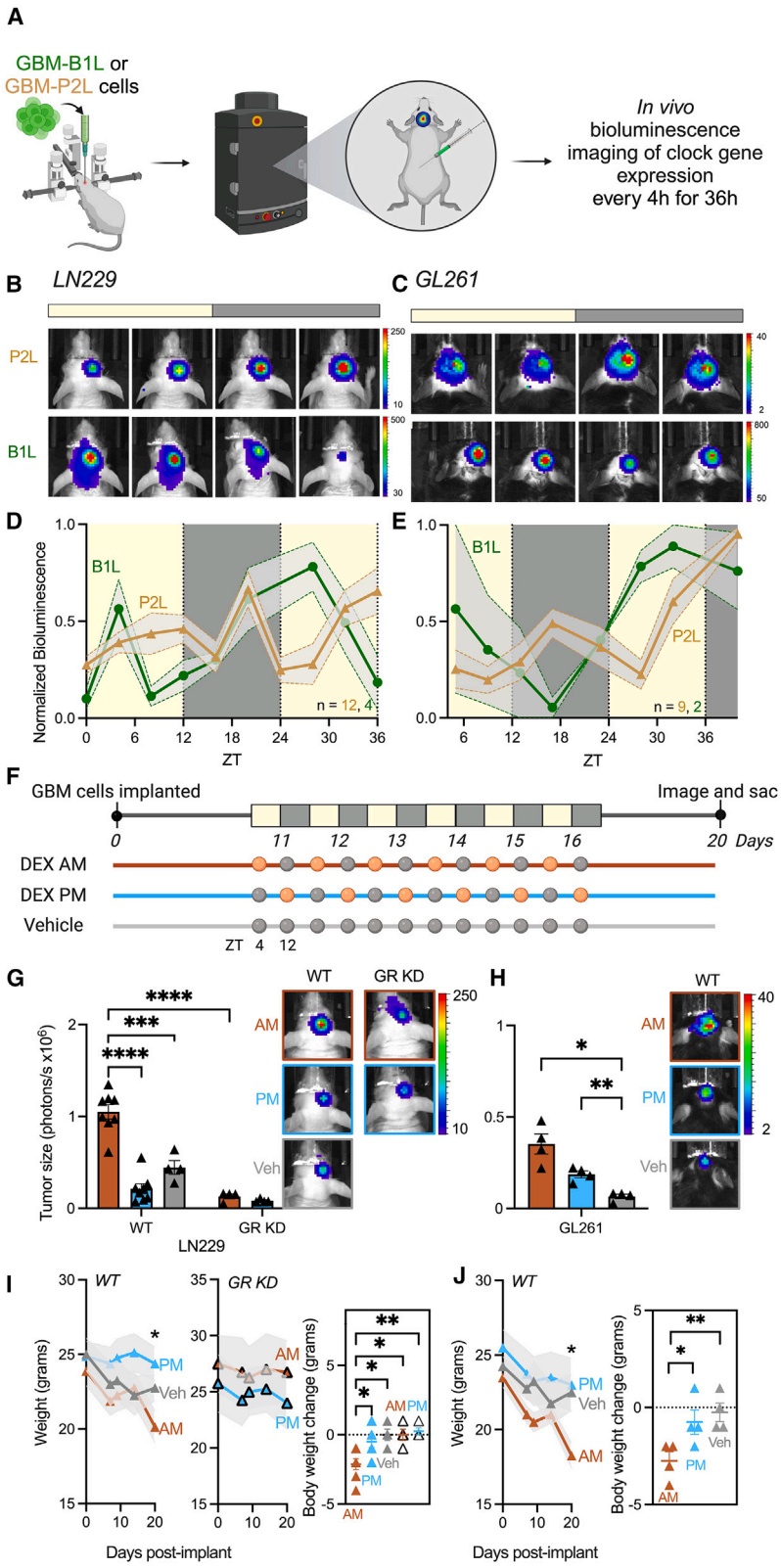

Figure 2. Dexamethasone promotes GBM growth through glucocorticoid receptor signaling when administered in the morning around the daily trough of *Per2* expression *in vivo*

(A) Schematic of orthotopic xenograft into mouse basal ganglia and bioluminescence imaging. Mice were implanted with GBM cells expressing a *Per2*:luc (P2L) or *Bmal1*:luc (B1L) reporter to record tumor clock gene expression.

(B and C) Representative bioluminescence images of LN229 (B) and GL261 (C) tumor xenografts in mice during the day (ZT0–12, yellow bar) and night (ZT12–24, gray bar) show high *Bmal1* expression during the day, and high *Per2* expression during the night (BLI counts are $\times 10^3$, color bar depicts relative bioluminescence intensity).

(D and E) GBM xenografts show reliable peak *Per2* (yellow line) expression at night and *Bmal1* (green line) during the day when implanted in nude (D) or C57BL/6NJ (E) male or female mice (zeitgeber time (ZT), mean ± SEM, *n* reported in figure, average traces scored circadian by JTK cycle $p < 0.05$). Light yellow background represents daytime and gray background represents nighttime.

(F) Schematic of two DEX treatment paradigms after tumor implantation. Each dot represents a time of treatment; orange dots represent treatment with DEX, while gray dots represent treatment with vehicle. Yellow bars represent daytime and gray bars represent nighttime.

(G and H) DEX in the morning promotes LN229 (G) and GL261 (H) tumor growth *in vivo*. Tumor size increased 2- to 5-fold when treating mice implanted with wild-type (WT) LN229 or GL261 cells in the morning (ZT4, AM) compared to evening (ZT12, PM) or vehicle (Veh). DEX in the morning or evening did not significantly induce tumor growth in mice implanted with GR KD LN229 cells (mean ± SEM, $n = 8$ in WT LN229-bearing mice receiving DEX AM or PM, $n = 4$ in all other groups, BLI counts on representative images are $\times 10^3$, color bar depicts relative bioluminescence, one-way ANOVA with Tukey's multiple comparisons test, $^*p < 0.05$, $^{**}p < 0.01$, $^{***}p < 0.001$, $^{****}p < 0.0001$).

(I) Mice bearing LN229 WT tumors treated with DEX in the morning lost more body weight from start to end of the experiment compared to mice treated in the evening or with vehicle, or bearing GR KD cells (mean ± SEM, $n = 4$ per group, left: two-way ANOVA with Tukey's multiple comparisons test, right: one-way ANOVA with Tukey's multiple comparisons test, $^*p < 0.05$, $^{**}p < 0.01$).

(J) Mice bearing GL261 WT tumors treated with DEX in the morning lost more body weight from start to end of the experiment compared to mice treated in the evening or with vehicle (mean ± SEM, $n = 4$ per group, left: two-way ANOVA with Tukey's multiple comparisons test, right: one-way ANOVA with Tukey's multiple comparisons test, $^*p < 0.05$, $^{**}p < 0.01$). See also Figures S3–S6.

Please cite this article in press as: Gonzalez-Aponte et al., Daily glucocorticoids promote glioblastoma growth and circadian synchrony to the host, Cancer Cell (2024), https://doi.org/10.1016/j.ccell.2024.11.012

CellPress
OPEN ACCESS

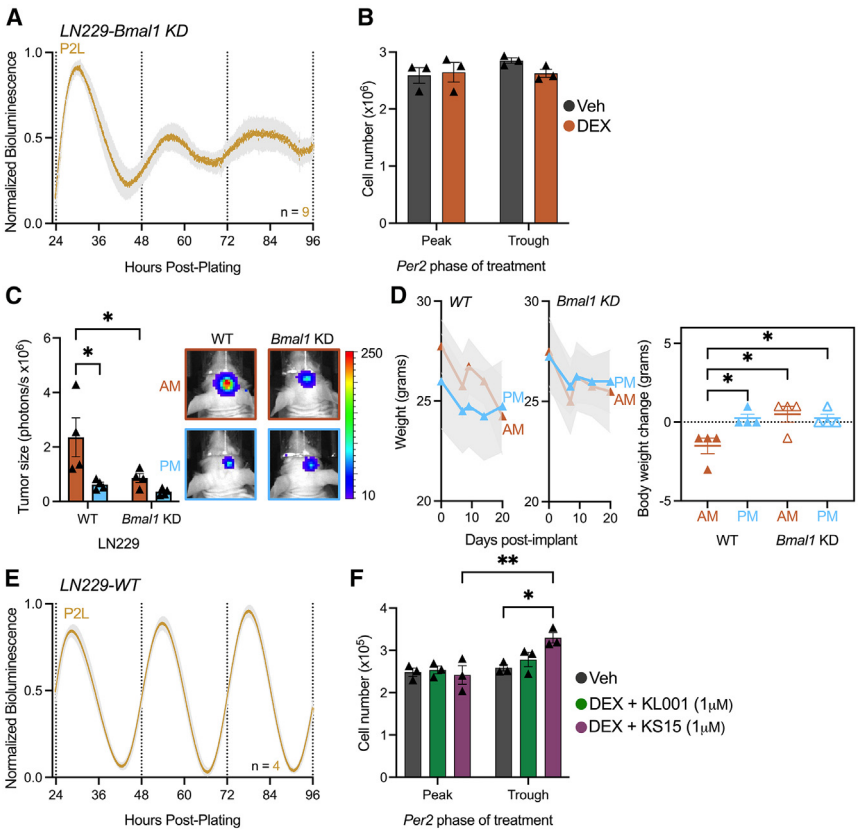

Figure 3. Dexamethasone-induced growth (around the daily trough of *Per2* or morning) and suppression (around the daily peak of *Per2* or evening) depends on an intact circadian clock in GBM cells

(A) *BMAL1* KD reduced the amplitude of daily rhythms in *Per2* in human LN229-P2L cells *in vitro* (hereafter abbreviated as *Bmal1* KD, shRNA construct 14, mean ± SEM, *n* reported in figure, all recordings had cosine fits with correlation coefficients of CC < 0.7 *Bmal1* KD).

(B) LN229-P2L cells with *Bmal1* KD showed no differences in growth in response to 100 nM DEX or vehicle treatment around the peak or trough of *Per2* expression *in vitro* (mean ± SEM, $n = 3$ per group, two-way ANOVA with Šídák's multiple comparisons test, ns $p > 0.05$).

(C) DEX increased growth by about 3-fold when administered in the morning (ZT4, AM) compared to the evening (ZT12, PM) *in vivo*. No significant differences in tumor size were observed in mice bearing LN229 *Bmal1* KD tumors, or treated with DEX in the morning or evening (mean ± SEM, $n = 4$ per group, BLI counts on representative images are $\times 10^3$, color bar depicts relative bioluminescence, one-way ANOVA with Tukey's multiple comparisons test, $^*p < 0.05$).

(D) Mice bearing LN229 WT tumors treated with DEX in the morning (orange) lost more weight from start to end of the experiment compared to mice treated in the evening (blue), or bearing an LN229 *Bmal1* KD tumor (mean ± SEM, $n = 4$ per group, left: two-way ANOVA with Tukey's multiple comparisons test, right: one-way ANOVA with Tukey's multiple comparisons test, $^*p < 0.05$).

(E) Human LN229-P2L GBM cells show circadian rhythms in *Per2* gene expression *in vitro* (mean ± SEM, *n* reported in figure, all recordings had cosine fits with correlation coefficients of CC > 0.9).

(F) Treatment with a cryptochrome agonist (KL001, 1 μM) also blocked the time-of-day dependent growth response to DEX *in vitro*. In contrast, a cryptochrome inhibitor (KS15, 1 μM) increased cell growth to DEX at the trough, but not at the peak, of *Per2* expression compared to vehicle (mean ± SEM, $n = 3$ per group, two-way ANOVA with Šídák's multiple comparisons test, $^*p < 0.05$, $^{**}p < 0.01$). See also Figure S7.

indicator of tumor proliferation, we collected brain tissue at 20 days post-implant and stained for the proliferation marker Ki67. We found significantly higher Ki67 expression and tumor area in brain sections from mice receiving DEX in the morning, compared to evening or vehicle (Figure S6A and S6B). We conclude that glucocorticoids in the morning *in vivo* (around peak *Bmal1* and trough *Per2* expression) promote GBM growth and accelerate disease progression through intrinsic GR signaling.

Our results showing time- and GR-dependent effects of DEX on tumor growth suggest a circadian modulation of glucocorticoid signaling in GBM. To test whether the growth-promoting effects of DEX depend on an intact circadian clock, we used two different viral-mediated short hairpin RNA constructs to reduce *Bmal1* levels with an 86%–93% KD efficiency (Figure S7A). We found both KD constructs disrupted the intrinsic circadian clock, as evidenced by decreased amplitude of circadian *Per2* expression in LN229-P2L cells (Figure 3A, and S7B-C). We next treated LN229-P2L *Bmal1* KD cells with 100 nM DEX or vehicle at either the peak or trough of *Per2* expression. We found that *Bmal1* KD abolished DEX-induced tumor growth or suppression at both circadian phases *in vitro* (Figures 3B and S7D). To test this hypothesis *in vivo*, we implanted LN229 WT or *Bmal1* KD cells into the basal ganglia of immunocompromised nude mice, tracked tumor size by *in vivo* bioluminescence imaging, and delivered DEX or vehicle in the morning or evening for six days. Consistent with our previous findings, morning treatment with DEX significantly increased LN229 WT tumor size and mice lost more weight, compared to evening treatment (Figures 3C and 3D). In contrast, no differences in tumor size and body weight loss were found between morning and evening treatment groups in mice bearing LN229 *Bmal1* KD tumors (Figures 3C and 3D).

To further test whether the circadian clock regulates DEX-induced GBM growth, we modulated the activity of the clock repressor Cryptochrome (*Cry*) using the validated agonist (KL001) or inhibitor (KS15) of CRY1 and CRY2 proteins.[32,48–50] We treated LN229-P2L cells with either 100 nM DEX in combination with 1 μM KL001, 100 nM DEX in combination with 1 μM KS15, or vehicle, at either the peak or trough of *Per2* expression (Figure 3E). We found that KL001 abrogated the time-dependent growth and suppressive responses to DEX *in vitro* at both phases of *Per2* expression (Figure 3F). In contrast, KS15 blocked the suppressive effect of DEX at peak *Per2* and sustained DEX-induced cell growth at the trough of *Per2* expression compared to vehicle (Figure 3F). We conclude that the circadian clock in

Please cite this article in press as: Gonzalez-Aponte et al., Daily glucocorticoids promote glioblastoma growth and circadian synchrony to the host, Cancer Cell (2024), https://doi.org/10.1016/j.ccell.2024.11.012

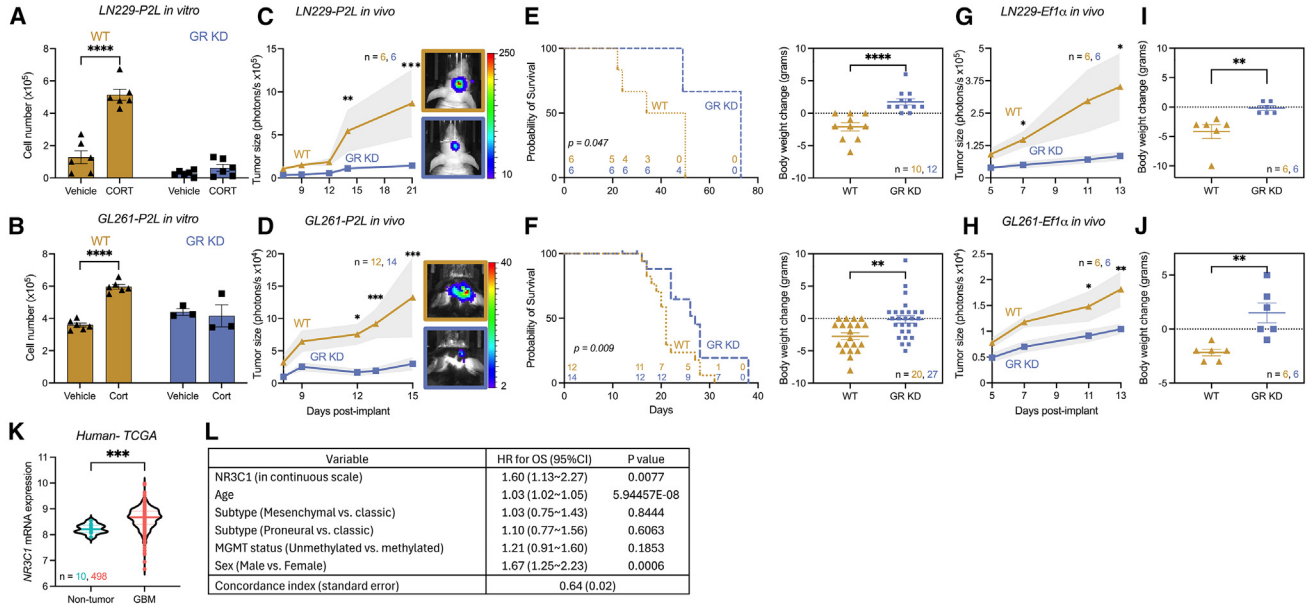

L

Variable	HR for OS (95%CI)	P value
NR3C1 (in continuous scale)	1.60 (1.13~2.27)	0.0077
Age	1.03 (1.02~1.05)	5.94457E-08
Subtype (Mesenchymal vs. classic)	1.03 (0.75~1.43)	0.8444
Subtype (Proneural vs. classic)	1.10 (0.77~1.56)	0.6063
MGMT status (Unmethylated vs. methylated)	1.21 (0.91~1.60)	0.1853
Sex (Male vs. Female)	1.67 (1.25~2.23)	0.0006
Concordance index (standard error)	0.64 (0.02)	

Figure 4. Daily glucocorticoid signaling promotes GBM growth and accelerates disease progression

(A and B) Glucocorticoids promote cell growth *in vitro* in LN229 (A) and GL261 (B) WT, but not in GR KD cells (mean ± SEM, $n = 3$ for GR KD GL261-P2L cells, $n = 6$ in all other groups. Two-way ANOVA with Bonferroni's multiple comparisons test, $^{****}p < 0.0001$, ns $p > 0.05$). Cells treated with 100 μM cortisol (LN229) or corticosterone (GL261) (Cort) grew an average of 4- to 2-fold compared to vehicle-treated or GR KD cultures.

(C and D) Tumor size was higher in mice bearing LN229 (C) and GL261 (D) WT tumors (yellow) compared to GR KD (blue, mean ± SEM, *n* reported in figure, two-way ANOVA with Šídák's multiple comparisons test, $^{*}p < 0.05$, $^{**}p < 0.01$, $^{***}p < 0.001$. BLI counts on representative images are $\times 10^3$, color bar depicts relative bioluminescence).

(E and F) Probability of survival was higher in mice bearing LN229 (E) and GL261 (F) GR KD tumors compared to those implanted with WT tumors (*n* reported in figure, log rank Mantel-cox test, $^{*}p < 0.05$. Mice bearing LN229 (E) or GL261 (F) GR KD tumors lost less weight from start to the end of the experiment compared to mice implanted with WT tumors (mean ± SEM, *n* reported in figure, Student's t test, $^{**}p < 0.01$, $^{****}p < 0.0001$).

(G and H) Independent measurements of tumor size using a constitutive *Ef1a*-luc reporter in LN229 (G) and GL261 (H) tumors showed higher tumor bioluminescence in mice bearing WT tumors (yellow) compared to GR KD (blue, mean ± SEM, *n* reported in figure, two-way ANOVA with Šídák's multiple comparisons test, $^{*}p < 0.05$, $^{**}p < 0.01$).

(I and J) Mice bearing LN299 (I) and GL261 (J)-*Ef1a* GR KD tumors lost less weight from start to the end of the experiment compared to mice implanted with WT tumors (mean ± SEM, *n* reported in figure, Student's t test, $^{**}p < 0.01$).

(K) *NR3C1* (GR) mRNA expression was significantly higher in human IDH1 WT GBM samples compared to non-tumor histology (data obtained from The Cancer Genome Atlas Program (TCGA) database, *n* reported in figure, solid line indicates median, Wilcoxon rank-sum test, $^{***}p < 0.001$).

(L) Cox proportional hazard model on patients' overall survival with NR3C1, with incorporation of known risk factors, showed a 60% increase in hazard of mortality for every one unit increase in NR3C1 expression in GBM (Wald test, abbreviations in table are defined as follows: hazard ratio (HR), overall survival (OS), confidence interval (CI), O6-methylguanine-DNA methyltransferase (MGMT). See also Figures S8 and S9.

GBM cells is necessary for DEX-induced growth around the daily *Per2* trough (morning) and suppression around the daily *Per2* peak (evening).

We propose a model whereby during the night, when the clock repressors *Per* and *Cry* are highly expressed in GBM cells, GR signaling activity is repressed by the circadian clock, leading to GBM growth arrest or suppression. In contrast, during the morning, when expression of *Per* and *Cry* decreases, and the clock activator *Bmal1* increases, GR signaling is enabled to respond to circulating glucocorticoids, promoting GBM growth.

Daily glucocorticoid signaling to GBM promotes tumor growth and accelerates disease progression

To test the hypothesis that daily endogenous glucocorticoid signaling regulates GBM progression, we first treated LN229-P2L and GL261-P2L cells, with or without GR, with the glucocorticoids cortisol and corticosterone, respectively. Consistent with our previous findings using the synthetic glucocorticoid DEX, treating GBM cells with corticosterone or cortisol resulted in increased cell growth, compared to vehicle (Figures 4A and 4B). Knocking down GR eliminated glucocorticoid-induced cell growth (Figures 4A and 4B), suggesting that glucocorticoids must act through GR to promote GBM growth. We next implanted LN229-P2L and GL261-P2L cells, WT or GR KD, into the basal ganglia of immunocompromised nude or C57 WT mice, respectively. *In vivo*, GR KD tumors grew strikingly less, by 5- to 6-fold, than WT tumors (Figures 4C and 4D) and these mice survived longer and lost less weight from start to end of the experiment (Figures 4E and 4F). As an independent assessment of tumor progression *in vivo*, we measured expression of the constitutive reporter *Ef1a*:luc in GBM xenografts. We found *Ef1a*-driven bioluminescence in LN229 and GL261 cells increased with cell number, without circadian modulation, *in vitro* (Figures S8A and S8B), and *in vivo* (Figures S8C and S8D). We next generated GR KD lines of LN229- and GL261-*Ef1a*:luc cells and tracked tumor size following implantation

Please cite this article in press as: Gonzalez-Aponte et al., Daily glucocorticoids promote glioblastoma growth and circadian synchrony to the host, Cancer Cell (2024), https://doi.org/10.1016/j.ccell.2024.11.012

CellPress
OPEN ACCESS

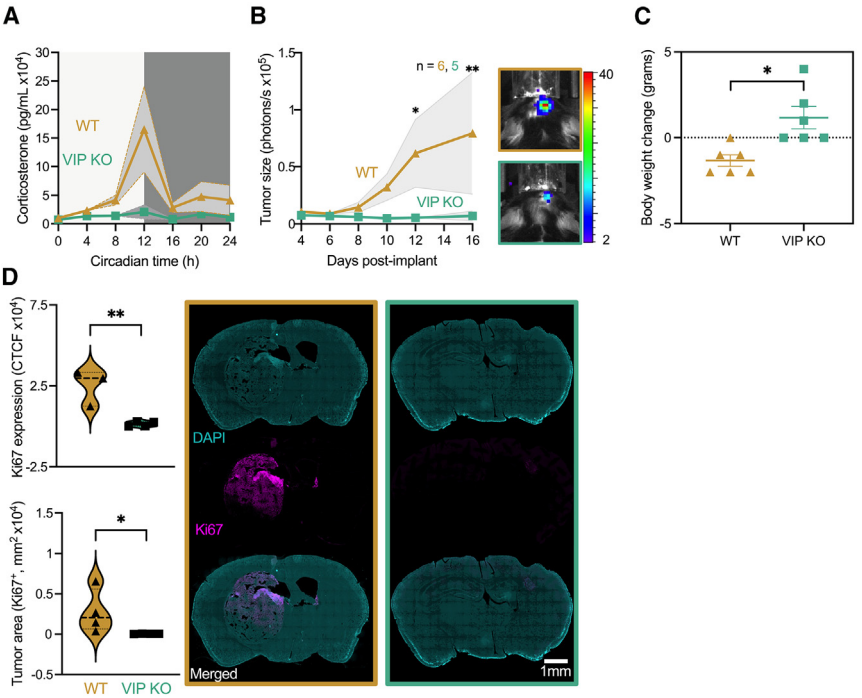

Figure 5. Disruption of circadian rhythms in the host slows GBM growth and disease progression

(A) Fecal corticosterone (CORT) concentration was circadian in WT, but not VIP KO mice (mean ± SEM, $n = 3$ per group, WT trace scored circadian by JTK cycle $p < 0.05$).

(B) Tumor size was higher in WT mice bearing GL261 tumors compared to VIP KO mice (mean ± SEM, n reported in figure, two-way ANOVA with Šídák's multiple comparisons test, $^{*}p < 0.05$, $^{**}p < 0.01$. BLI counts on representative images are $\times 10^3$, color bar depicts relative bioluminescence).

(C) VIP KO mice bearing GL261 tumors lost less weight from start to the end of the experiment compared to WT mice (mean ± SEM, $n = 6$ per group, Student's t test, $^{*}p < 0.05$).

(D) GBM proliferation and tumor area, as measured by Ki67 expression, was higher in WT mice bearing GL261 tumors (images with yellow frame) compared to VIP KO mice (images with green frame). In violin plots, dotted lines indicate 25th and 75th percentile, solid line indicates 50th percentile (median). (Scale bar: 1 mm, $n = 4$ per group, Student's t test, $^{*}p < 0.05$, $^{**}p < 0.01$). Composite images of DAPI to label cell nuclei (blue) and Ki67 (magenta) immunostaining of brain sections reveal tumor location and size.

into the basal ganglia. Consistent with our previous findings, GR KD cells grew significantly less, by 2- to 5-fold, than WT xenografts (Figures 4G and 4H). These mice lost less weight from start to end of the experiment, indicating slower disease progression (Figures 4I and 4J). Finally, we measured Ki67 expression as an additional marker of cell proliferation and found significantly higher Ki67 expression and tumor area in WT tumor slices, compared to GR KD (Figures S9A and S9B). These results indicate that GR expression in GBM cells is required for endogenous glucocorticoids to promote tumor growth and disease progression.

To assess the potential clinical significance of targeting the glucocorticoid signaling pathway in GBM, we analyzed expression of *NR3C1* (GR) in GBM patient samples using data from The Cancer Genome Atlas (TCGA). We found that *NR3C1* mRNA levels were significantly higher in GBM relative to non-tumor histology (Figure 4K). To investigate the impact of *NR3C1* expression on GBM patient survival, we fit a Cox proportional hazard model on patients' overall survival and found that hazard of mortality significantly increased by 60% for every one unit increase in *NR3C1* expression in GBM (Figure 4L). These data support that targeting the glucocorticoid receptor signaling pathway could be a promising strategy for treating GBM patients.

To further evaluate if daily rhythms in glucocorticoid secretion regulate GBM progression, we implanted GL261-P2L cells into the basal ganglia of mice with impaired circadian rhythms. We chose to study mice with the VIP gene knocked out because they lose circadian regulation of rest-wake activity and corticosterone secretion.[40,51] We measured fecal corticosterone every 4 h for 24 h in WT and VIP KO mice bearing GL261-P2L tumors and housed in constant darkness.[29] We found corticosterone secretion peaked during the subjective night (CT12) in WT but remained chronically low in VIP KO mice (Figure 5A). GBM tumors grew more in WT mice, by 11-fold, compared to VIP KO (Figure 5B). Furthermore, VIP KO mice bearing GL261-P2L tumors gained body weight from start to end of the experiment, whereas WT mice lost weight (Figure 5C), demonstrating that circadian signaling is required for aggressive GBM progression. Finally, we found significantly higher Ki67 expression and tumor area in tumors implanted into WT mice, compared to VIP KO (Figure 5D). Altogether, these results suggest that the daily surge in glucocorticoid secretion around waking promotes GBM growth and accelerates disease progression.

Intrinsic daily rhythms of mouse and human GBM cells synchronize to the host's central clock

To assess if GBM cells implanted into the basal ganglia act as circadian pacemakers that entrain to daily local cues, we recorded *Bmal1* expression from NF1$^{-/-}$DNp53 and running wheel activity of mice 2 weeks after reversing the 12 h:12 h light:dark cycle (LD to DL, lights on 7 p.m.–7 a.m.; Figure 6A). We found that, before the shift in the light cycle, tumor *Bmal1* expression peaked around ZT4 (8 h before daily locomotor activity onset) and *Per2* peaked around ZT18 (6 h after activity onset) in individual mice and group averages (Figures 6B and 6C). After 2 weeks in the reversed light schedule, tumor daily rhythms showed peak *Bmal1* around ZT0 and *Per2* around ZT13 (Figures 6D and 6E). We then evaluated these mice after 2 weeks in constant darkness (DD) and found that tumor rhythms shifted with the free-running period of locomotor activity of each mouse (*Bmal1* peaked at CT2 and *Per2* peaked at CT14; Figures 6F and 6G). These findings suggest that clock gene expression in GBM tumors entrains to the host's central clock, shifting as mice entrain to changes in the light cycle.

To further evaluate how daily rhythms in brain tumors entrain to the host, we implanted GL261-P2L GBM cells into the basal

Please cite this article in press as: Gonzalez-Aponte et al., Daily glucocorticoids promote glioblastoma growth and circadian synchrony to the host, Cancer Cell (2024), https://doi.org/10.1016/j.ccell.2024.11.012

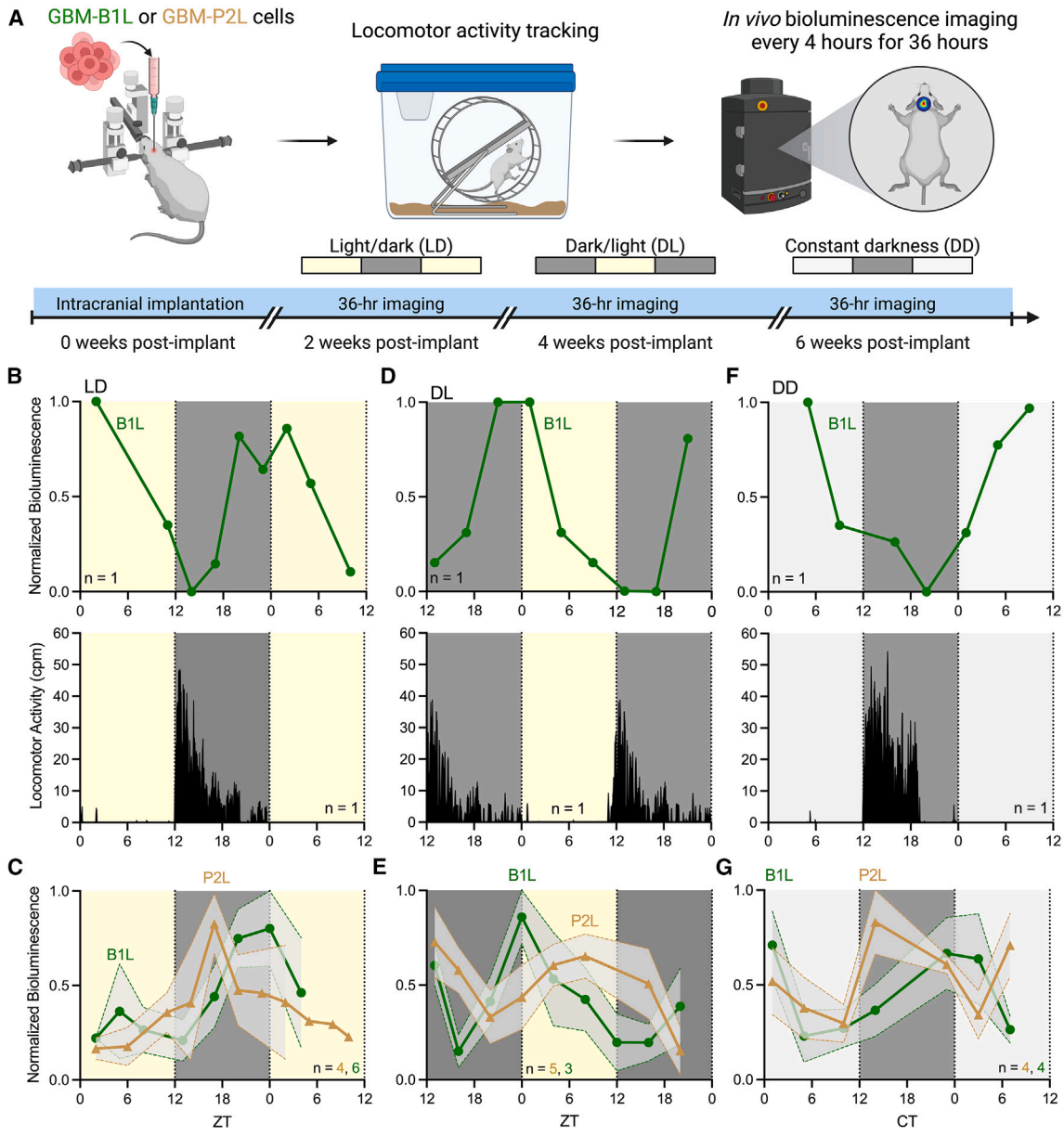

Figure 6. Peak timing of tumor *Bmal1* and *Per2* synchronizes to host rest-wake activity in different light cycles

(A) Schematic of light shifting paradigm after tumor implantation. Mice were housed in standard 12:12 light/dark conditions (LD), reversed 12:12 dark/light (DL), or constant darkness (DD). Light yellow background represents daytime and gray background represents nighttime.

(B) Representative 36-h *in vivo* bioluminescence imaging (top) and locomotor activity profile (bottom) of a mouse implanted with NF1$^{-/-}$ DNp53-B1L cells, in a standard 12L:12D light schedule, two weeks post-implant, showed peak *Bmal1* expression during the light phase (trace scored circadian by JTK cycle $p < 0.05$) and entrainment to the light cycle. Light yellow background represents daytime and gray background represents nighttime.

(C) Average traces of 36-h *in vivo* imaging of NF1$^{-/-}$ DNp53-B1L (green line) and -P2L (yellow line) GBM tumors two weeks post-implant, in a standard 12L:12D light schedule, showed peak *Bmal1* during the light phase and *Per2* during the dark phase (mean ± SEM, *n* reported in figure, average traces scored circadian by JTK cycle $p < 0.05$). Light yellow background represents daytime and gray background represents nighttime.

(D) 36-h *in vivo* imaging (top) and locomotor activity profile (bottom) of the same mouse after two weeks in a reversed 12L:12D light schedule, four weeks post-implant, showed *Bmal1* synchronized to the new dark-light cycle, peaking during the light phase (trace scored circadian by JTK cycle $p < 0.05$). Light yellow background represents daytime and gray background represents nighttime.

(E) Average traces of 36-h *in vivo* imaging of NF1$^{-/-}$ DNp53-B1L (green line) and -P2L (yellow line) GBM tumors after two weeks in a reversed 12L:12D light schedule (four weeks post-implant) showed tumor rhythms synchronized to the new light-dark schedule (mean ± SEM, *n* reported in figure, average traces scored circadian by JTK cycle $p < 0.05$). Light yellow background represents daytime and gray background represents nighttime.

(F) 36-h *in vivo* imaging (top) and locomotor activity profile (bottom) of the same mouse after two weeks in constant darkness (six weeks post-implant) showed *Bmal1* peaking with the offset of daily locomotion (trace scored circadian by JTK cycle $p < 0.05$). Light gray background represents subjective daytime, and dark gray background represents subjective nighttime.

(legend continued on next page)

ganglia of WT and VIP KO mice, and recorded locomotor activity and GBM clock gene expression. We found that, in individual WT mice, *Per2* reliably peaked at night (CT16), about 4 h after daily locomotor onset, but peaked at random times in individual VIP KO mice that lacked daily rhythms in locomotion (Figures 7A, 7B, and S10A–S10H). Thus, group averaged *Per2* expression was circadian in WT (Figures 7C and S10A–S10D), but not in VIP KO mice (Figures 7D and S10E–S10H). We used the time of daily peak *Per2* expression from the GBM xenograft of each mouse to quantify the high synchrony among tumors in WT, but not VIP KO mice (Figures S10I–S10K). Altogether, our findings indicate daily rhythms in the host are required to synchronize tumor daily *Per2* expression. We conclude that GBM tumors act as peripheral circadian oscillators that synchronize to the host's central clock.

GBM requires glucocorticoid receptors to synchronize daily rhythms to the host

Cell-autonomous circadian clocks have been found in brain regions outside the central pacemaker in the SCN, including the olfactory bulb, pineal gland, and pituitary,[52–54] as well as outside the brain, in the liver, kidney, lung, brown fat, heart, adrenal gland, among others.[55–59] These peripheral oscillators likely integrate signals from the central circadian clock in the SCN to regulate daily rhythms in cellular processes. Candidate signals that have been found to synchronize peripheral clocks include insulin/IGF in combination with glucose, daily fluctuations in body temperature, and the daily secretion of glucocorticoids. Of these, glucocorticoids can synchronize circadian clocks in peripheral tissues and, since we found that tumors fail to entrain normally in VIP KO mice with blunted sleep-wake and glucocorticoid rhythms, we hypothesized that daily glucocorticoids suffice to synchronize daily rhythms in GBM to the host. To test this hypothesis, we recorded *Per2* expression *in vitro* from LN229- and GL261-P2L cells, WT or GR KD, treated with 100 nM DEX. We found that DEX rapidly induced *Per2* expression and shifted the daily rhythms in WT, but not GR KD, cells (Figures 8A–8D). On the second day after treatment, DEX delayed *Per2* peak expression in LN229-P2L cells by 4 h, compared to vehicle (0.001% ethanol), and by 5 h in GL261-P2L. Because DEX has a long half-life and thus can have lasting effects on daily gene expression, we next tested whether daily glucocorticoids can entrain GBM cultures. We recorded *Per2* expression from LN229 and GL261 cells *in vitro* and found that addition of glucocorticoids (100 μM cortisol or corticosterone) at CT0 for 3 consecutive days synchronized the time of daily peak *Per2* expression to a 24 h rhythm compared to vehicle (0.001% ethanol; Figures S11A–S11D). Cultures resumed their free-running circadian periods after termination of daily glucocorticoid administration. Together, these findings suggest that daily glucocorticoid treatment entrains intrinsic *Per2* expression in GBM *in vitro*.

To test if GR signaling coordinates GBM circadian rhythms *in vivo*, we next recorded clock gene expression from GR-deficient xenografts in tumor-bearing mice. We implanted WT or GR KD GBM cells into the basal ganglia of mice (LN229-P2L into immunocompromised nude or GL261-P2L into C57 WT). After recovery and detection of bioluminescence over background, we monitored *Per2*-driven bioluminescence every 4 h for 36 h (Figures 8E and 8F). We found tumor *Per2* expression reliably peaked in the middle of the night (ZT12–20) in LN229 and GL261 WT cells but peaked at varying times of day in GR-deficient GBM cells, as evidenced by a lower synchronization index among mice and misalignment with the daily locomotor activity onset (Figures 8G and 8H, and S12A–S12L). Additional real-time recordings of *Per2* expression from GL261 WT or GR KD xenografts in freely moving mice also revealed WT tumors peaked during the subjective night (CT16–19), but GR KD tumors peaked during the subjective day (CT5–6; Figures S12M–S12O). We conclude that glucocorticoid receptor signaling establishes a reliable time of daily clock gene expression in GBM *in vivo* and that blocking glucocorticoid signaling to the tumor impairs GBM circadian entrainment.

DISCUSSION

Previous research has centered on whether synthetic glucocorticoids like DEX regulate GBM progression, yet no studies have considered the role of daily rhythms in glucocorticoid signaling. Our findings identify daily rhythms in glucocorticoid signaling as a regulator of GBM progression, with DEX in the morning (around the daily peak of tumor *Bmal1* expression) promoting, and DEX in the evening (around the daily peak of tumor *Per2* expression) suppressing growth, *in vitro* and *in vivo*. Changes in body weight were consistent with morning DEX accelerating disease progression, compared to evening or vehicle treatments. These effects depended on activity of the glucocorticoid receptor (GR) and core clock genes *Bmal1* and *Cryptochrome* (*Cry*) *1* and *2*. We also found smaller tumors, longer host survival, and less body weight loss in mice bearing GBM tumors that lacked the glucocorticoid receptor (i.e., GR KD), suggesting that circadian regulation of glucocorticoid signaling in GBM directly drives daily tumor progression in response to endogenous glucocorticoids or exogenously delivered glucocorticoids like DEX.

The higher expression of GR and increased hazard of mortality with increased GR expression in human GBM patient samples further implicates the GR signaling pathway as a potential target for therapy. Because we found that mice lacking a daily surge in glucocorticoids (i.e., VIP KO) had slower growing GBM tumors, we propose that treatments that suppress the activation of the GR signaling pathway will be effective therapies against GBM progression.

The finding that daily glucocorticoid signaling promotes GBM growth opens the doors to a deeper mechanistic understanding of its role in glioma tumorigenesis and progression. Glucocorticoids maintain various metabolic and homeostatic functions by binding to the glucocorticoid receptor. In the absence of

(G) Average traces of 36-h *in vivo* imaging of NF1$^{-/-}$ DNp53-B1L (green line) and -P2L (yellow line) GBM tumors after two weeks in constant darkness (six weeks post-implant) showed peak expression of *Per2* aligned with subjective dusk and *Bmal1* with subjective dawn (mean ± SEM, *n* reported in figure, average traces scored circadian by JTK cycle $p < 0.05$, circadian time 12, CT12, based on daily locomotor activity onset). Light gray background represents subjective daytime, and dark gray background represents subjective nighttime.

Please cite this article in press as: Gonzalez-Aponte et al., Daily glucocorticoids promote glioblastoma growth and circadian synchrony to the host, Cancer Cell (2024), https://doi.org/10.1016/j.ccell.2024.11.012

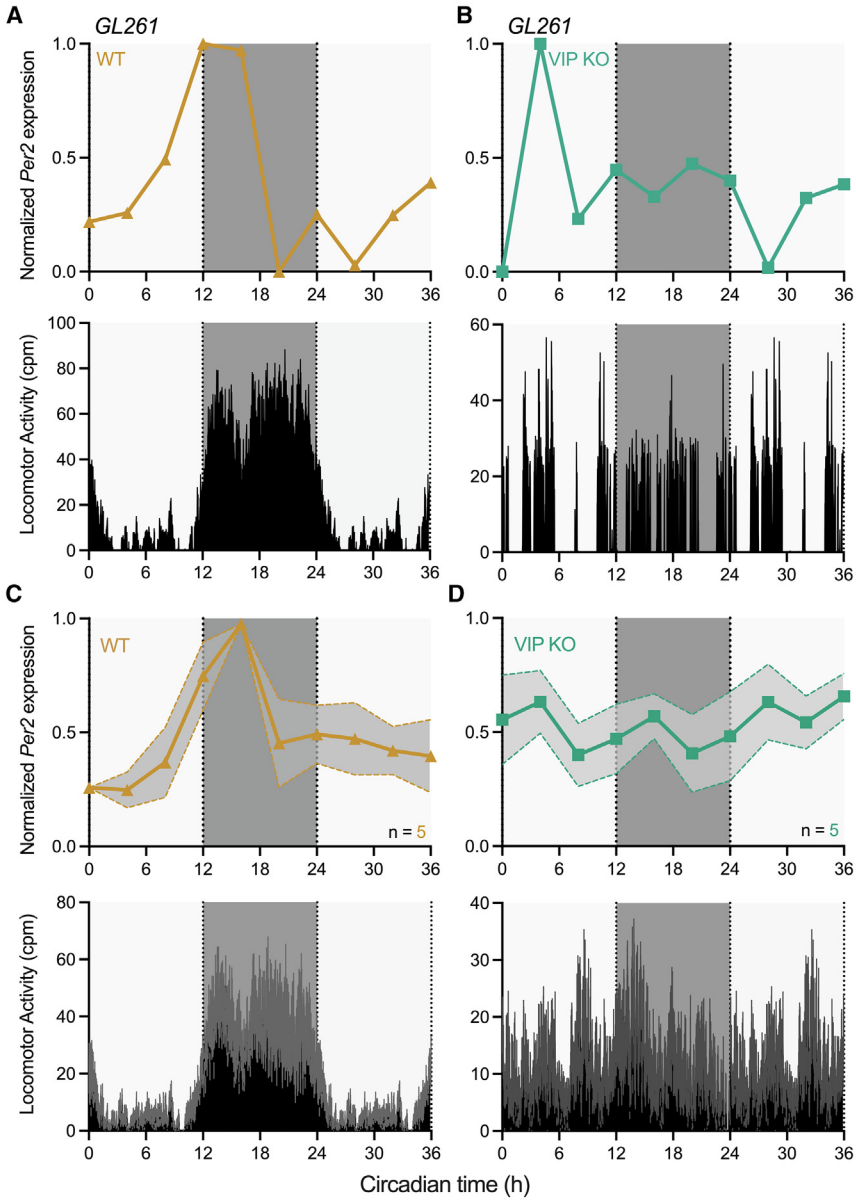

Figure 7. Disruption of daily rhythms in the host desynchronizes tumor *Per2* expression from the host rest-wake activity

(A) Representative 36-h *in vivo* bioluminescence imaging (top) and locomotor activity profile (bottom) of a WT mouse implanted with GL261-P2L cells, two weeks post-implant and in constant darkness showed tumor *Per2* expression peaking during the subjective dark phase (circadian time [CT] 16, trace scored circadian by JTK cycle $p < 0.05$) and rhythmic locomotor activity starting at CT12. Light gray background represents subjective daytime, and dark gray background represents subjective nighttime.

(B) Representative 36-h *in vivo* bioluminescence imaging (top) and locomotor activity profile (bottom) of a VIP KO mouse implanted with GL261-P2L cells, two weeks post-implant and in constant darkness, showed tumor *Per2* expression peaking during the subjective light phase (CT4, trace scored circadian by JTK cycle $p < 0.05$) and arrhythmic locomotor activity patterns. Light gray background represents subjective daytime, and dark gray background represents subjective nighttime.

(C) Average trace of 36-h *in vivo* imaging of WT mice (top) and average locomotor activity profiles (bottom) for all mice implanted with GL261-P2L tumors, two weeks post-implant and in constant darkness (subjective day = light gray and subjective night = dark gray background), showed reliable *Per2* peak expression and rhythmic daily activity (mean ± SEM, *n* reported in figure, average trace scored circadian by JTK cycle $p < 0.05$).

(D) Average trace of 36-h *in vivo* imaging of VIP KO mice (top) and average locomotor activity profiles (bottom) for all mice implanted with GL261-P2L tumors, two weeks post-implant and in constant darkness, showed desynchronized *Per2* peak timing and arrhythmic daily activity (mean ± SEM, *n* reported in figure, average trace not scored circadian by JTK cycle $p > 0.05$). Light gray background represents subjective daytime, and dark gray background represents subjective nighttime. See also Figure S10.

glucocorticoids, GR is localized to the cytoplasm, bound to chaperone proteins such as HSP90. Upon ligand binding, GR undergoes a confirmational change that triggers its translocation to the nucleus, where it can exert its actions primarily through genomic transactivation and transrepression, or by non-genomic signaling mechanisms.[60] The mechanisms by which this signaling program is regulated by the circadian clock include the circadian repressors *Cryptochromes* 1 and 2, which both bind GR in a ligand-dependent manner and repress GR expression at night to modulate transcriptional response to glucocorticoids.[31] Further, we found that GR gene expression varies with circadian time *in vitro* in GBM cells, suggesting that one mechanism by which the clock could regulate response to glucocorticoids is through direct regulation of GR transcription as a function of time of day. It will be important to learn how circadian signals within GBM and between cells in the tumor microenvironment regulate the response to glucocorticoids in GBM to elucidate additional therapeutic targets and best times for treatment of GBM.

Beyond regulating normal tissue function, the role of GR in cancer has been understudied beyond murine lymphoma, human leukemia cells, mouse primary thymocytes, human primary chronic lymphoblastic leukemia, and acute lymphoblastic leukemia, in which GR acts as a proapoptotic cue.[61–65] In other cell types, however, GR has been shown to coordinate cell division and mitosis, with loss of GR leading to aberrant chromosome segregation, accumulation of chromosome complement defects, and a robust mitotic phenotype.[66] While the role of GR in GBM has received very little attention, our findings suggest that this signaling pathway regulates tumor progression by inducing a proliferative phenotype, dependent on circadian clock regulation of GR signaling. We found that glucocorticoid-induced proliferation

Please cite this article in press as: Gonzalez-Aponte et al., Daily glucocorticoids promote glioblastoma growth and circadian synchrony to the host, Cancer Cell (2024), https://doi.org/10.1016/j.ccell.2024.11.012

CellPress
OPEN ACCESS

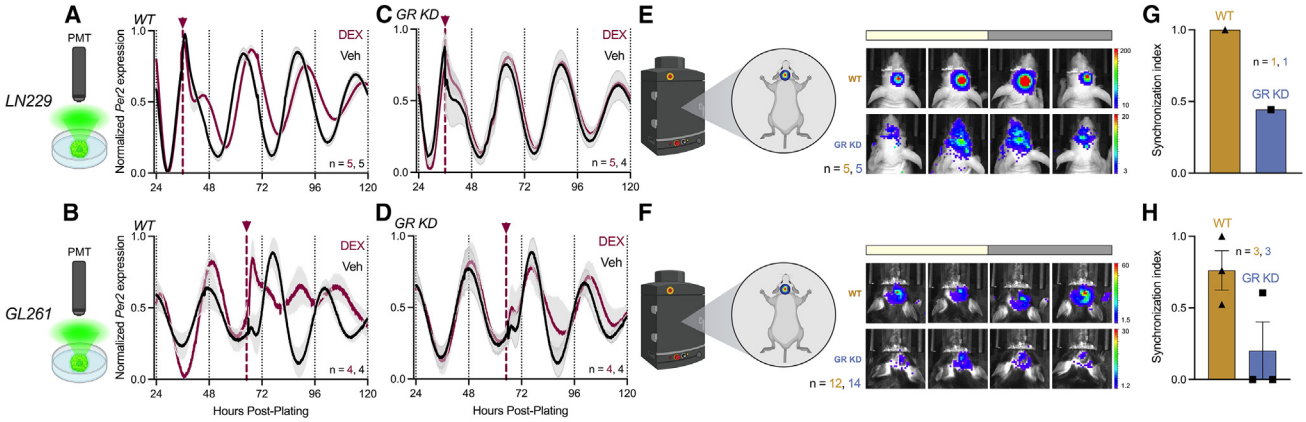

Figure 8. Timing of daily *Per2* expression in GBM xenografts depends on glucocorticoid receptor signaling

(A and B) Addition of 100 nM DEX shifted circadian *Per2* expression compared to vehicle in LN229 (A) and GL261 (B) GBM cells. Dashed line indicates time of DEX treatment, mean ± SEM, *n* reported in figure, all recordings had cosine fits with correlation coefficients, CC > 0.9).

(C and D) DEX did not phase shift *Per2* expression in GR KD LN229 (C) and GL261 (D) GBM cells. Dashed line indicates time of DEX treatment (mean ± SEM, *n* reported in figure, all recordings had cosine fits with correlation coefficients, CC > 0.9).

(E and F) Representative images of *in vivo* tumor imaging during the light (ZT0–12, yellow bar) and dark (ZT12–24, gray bar) phases of LN229-P2L (E) and GL261-P2L (F), WT or GR KD cells (BLI counts on representative images are $\times 10^3$, color bar depicts relative bioluminescence).

(G and H) Daily *Per2* profiles had high synchrony indices (i.e., peaked at similar times of day across mice) in LN229 (G) and GL261 (H) WT tumors. Synchrony was lower for tumors lacking GR (mean ± SEM, n reports cohort number. Synchronization index was calculated as an average of all mice in one cohort. In LN229, $n = 5$ mice per one WT or GR KD cohort. In GL261, $n = 12$ mice in 3 WT cohorts, and $n = 14$ mice in 3 GR KD cohorts). See also Figures S11 and S12.

depends on the clock genes *Bmal1* and *Cry*, which may relate to recent findings on glucocorticoid and circadian regulation of the cell cycle and metabolic homeostasis.[67–69] For example, a recent study found that DEX promotes GBM growth by downregulating genes controlling G2/M and mitotic-spindle checkpoints, and upregulating anti-apoptotic regulators BCL2L1 and MCL1.[67] It will be important to elucidate whether there are daily rhythms in activation of glucocorticoid response elements (GREs) and transactivation or transrepression of transcription that trigger cell proliferation in GBM. We propose that low PER and CRY expression, and high BMAL1 expression, facilitates activation of ligand-bound GR, which activates intrinsic signaling pathways that promote GBM growth. Thus, we predict treatments that augment PER or CRY activity, or inhibit BMAL1 activity, will suppress the growth-promoting effects of glucocorticoids like DEX. Future studies should test how the circadian clock modulates glucocorticoid and GR activity in GBM and examine which daily downstream signaling pathways are activated to regulate tumor growth.

Our findings support a model where GBM tumors act as peripheral circadian oscillators that can integrate into circadian circuits of the brain. This has implications for diagnosis and treatment. In the two human and two mouse GBM models tested *in vitro* and *in vivo*, regardless of sex or immune status of the host, *Bmal1* expression peaked during the day and *Per2* peaked at night, suggesting a conserved mechanism that synchronizes circadian rhythms across a variety of GBM cell types and genotypes. Recent findings in humans, cellular, and animal models of GBM have shown increased sensitivity to chemotherapy with TMZ when delivered in the morning.[6,8] This can now be explained based on the diversity of GBM models in this study that similarly entrain to the local light cycle in mice. This leads to the hypothesis that measuring daily rhythms in the host (e.g., sleep-wake or cortisol) could be used to guide optimized time of treatment for GBM.

How do brain cancers synchronize their daily rhythms to the host? We find, for example, that circadian gene expression in GBM xenografts adjusts to changes in the light cycle, synchronizes to daily rest-activity patterns, and depends on the neuropeptide, VIP, and daily hormones, such as glucocorticoids. One possibility is that SCN-driven signals dictate the internal phase of clock gene expression by acting as timing cues to peripheral oscillators. Multiple signaling pathways, such as calcium, cAMP, protein kinase A and C, VIP, glucocorticoids, and others, have been implicated in the regulation of phases of peripheral oscillators.[38,39,43,45,51,70–77]

Among mammalian peripheral tissues, manipulation of glucocorticoid signaling resets the phase of clock gene expression in the liver, heart, and kidney.[43] For example, the glucocorticoid receptor agonist DEX induces *Per1* gene expression in the liver, kidney, and rat primary hepatocytes, and downregulates *Reverbα* in liver tissues.[43] Here we found that DEX treatment shifts the phase of *Per2* gene expression in human and murine GBM cells *in vitro*, dependent on intact glucocorticoid receptor signaling. We present evidence that reveals that daily glucocorticoids synchronize daily rhythms in GBM tumors to the host, maintaining reliable clock gene expression patterns throughout the day. In the absence of glucocorticoid receptors or by disruption of glucocorticoid rhythms (i.e., VIP KO), GBM tumors sustain their daily rhythms, but *Per2* gene expression peaks at random times of day, suggesting that this peripheral signal acts as a time giver for the tumor. Our findings support a model whereby the master clock in the SCN regulates daily rhythms in glucocorticoid secretion that then synchronize daily clock gene expression in GBM tumors. Future studies should explore the mechanisms underlying how glucocorticoids and

Please cite this article in press as: Gonzalez-Aponte et al., Daily glucocorticoids promote glioblastoma growth and circadian synchrony to the host, Cancer Cell (2024), https://doi.org/10.1016/j.ccell.2024.11.012

other daily signals synchronize daily rhythms in GBM to the host.

Beyond maintaining synchronized daily rhythms between the tumor and the host, the circadian clock has been implicated in GBM tumorigenesis. For example, the CLOCK-BMAL1 complex promotes tumor angiogenesis and growth in GBM.[78,79] Disrupting the circadian clock by downregulating BMAL1 and CLOCK induces cell-cycle arrest and apoptosis in GBM stem cells.[32] In humans, analysis of TCGA data revealed that high expression of BMAL1 correlated with shorter patient survival times.[32] Altogether, these data led us to ask whether synchronized circadian rhythms drive GBM progression. We found that desynchronizing daily rhythms in GBM tumors from the host's clock by disrupting glucocorticoid receptor signaling significantly reduced tumor growth and slowed disease progression *in vivo*. Strikingly, tumors implanted into arrhythmic VIP KO mice, which also desynchronize from the host's central clock, fail to grow compared to tumors implanted into WT mice. Together, our findings suggest that synchronized circadian rhythms through glucocorticoid receptor signaling drive GBM progression.

Because of the localization of GBM tumors and their sensitivity to respond to peripheral signals, we do not exclude the possibility of other neural or non-neuronal signals acting as timing cues. Further, it is possible that timing cues also regulate glioma progression dependent on time of day. A wealth of recent data has presented evidence for a reciprocal crosstalk between gliomas and neurons in the tumor microenvironment that drives tumor progression.[80–86] Neuronal activity has been found to promote glioma growth,[83,84,86] while gliomas have been found to remodel adjacent neuronal synapses to induce a state of brain hyperactivity.[80,82,84,85] This raises the possibility that neuron-GBM communication synchronizes circadian rhythms in these tumors and promotes growth at specific times of day. Because neuronal activity and secretion of mitogens (i.e., neuroligin-3, semaphorin-4F, ephrinA6, and ephrinA7) varies with time of day,[81,87–91] it is possible that activity-driven glioma growth depends on circadian time. Outside of the brain, temperature, and insulin/IGF in combination with glucose can act as timing cues for many tissues.[41,42,45] Whether these signals promote daily GBM progression has not been studied. Future studies could test the role of brain temperature rhythms, and daily food intake and metabolism in tumor entrainment and growth. Moreover, future studies could focus on whether GBM is more sensitive to promitotic cues at specific times of day, if SCN and clock-derived signals regulate glioma progression, and whether neuron-GBM reciprocal crosstalk depends on circadian time. Altogether, this line of research will provide insights into how gliomas integrate into brain circuits, hijack its normal physiology, and use daily cues to grow. These findings could be leveraged to identify new therapeutic targets that can slow GBM progression, while opening avenues for treatment optimization by delivering therapies in accordance with a tumor's circadian rhythm.

The effects of DEX on GBM progression have remained controversial due to studies demonstrating anti- and pro-proliferative effects, depending on cell type, drug concentration and experimental conditions. Strikingly, many of these studies used the same GBM models and drug concentration but obtained opposite effects. DEX mimics the effects of endogenous glucocorticoids, a hormone secreted in a circadian fashion, by binding to glucocorticoid receptors (GRs) and activating this signaling pathway.[60,92] Non-concordance between previous studies could be the result of omitting circadian time of treatment as a biological variable underlying DEX effects on GBM progression. We identified circadian time as an important variable explaining the differential tumorigenic effects of DEX. These results suggest circadian regulation of the tumor's response to the synthetic glucocorticoid and represent a striking example of how chronotherapy (when a drug is delivered relative to circadian time) may differentially affect cancer outcomes.

Our findings have important implications for the use of DEX in GBM patients. Recent findings have demonstrated the potential benefits of circadian administration to maximize chemotherapy efficacy and tumor death in GBM (i.e., chronotherapy).[6–8,33] While it has not been studied for GBM, chronotherapy using corticosteroids has yielded positive effects for diseases like multiple sclerosis and rheumatoid arthritis.[93,94] Implementing a chronotherapeutic approach with DEX in the clinic may maximize its anti-inflammatory benefits while minimizing unwanted side effects including GBM growth. Because DEX may have a long half-life in brain (36–72 h),[95] it will be important to consider whether it or other corticosteroids, at specific times of day, associate with improved outcomes. If there is an optimal time of day for DEX to reduce edema and suppress tumor growth in patients, incorporating chronotherapy into the standard of care for DEX use in GBM patients requires no additional approvals or clinical trials.

Chronotherapy, also referred to as circadian medicine or chronomedicine, seeks to treat patients at the optimal time of day to maximize health benefits and minimize side effects. This approach has been shown to be effective in acute lymphoblastic leukemia,[96,97] colorectal,[98] ovarian, other gynecological cancers,[99] and most recently GBM,[6,8] but is neither the standard of care nor carefully evaluated in many cancers. We recently demonstrated that GBM cells and xenografts are more sensitive to TMZ when it is delivered at the daily peak of *Bmal1* clock gene expression *in vitro* and in the morning *in vivo*.[8] Daily sensitivity to TMZ is regulated by circadian expression of the DNA repair enzyme MGMT, and inhibiting its expression abolishes the daily rhythm in sensitivity to the drug.[8] In humans, timing TMZ to the morning extended patient survival by 6 months, compared to administering chemotherapy in the evening.[6] Here we found that, unlike some cancer types, GBM sustains intrinsic circadian rhythms that synchronize to the host and use daily clock-controlled cues to grow. Further, these daily rhythms can be leveraged to identify the best times of day to treat GBM tumors with drugs like TMZ and DEX.

Chronotherapy also considers daily signals, such as light in the morning and melatonin before sleep, as cues that synchronize a patient's daily rhythm. Previous findings show that tumor progression can be slowed by enhancing or inducing circadian rhythmicity in the host or in cancer tissues, such as breast,[100] melanoma,[101] colon carcinoma,[101] osteosarcoma,[102] and pancreatic adenocarcinoma.[103] To critically evaluate the potential for chronotherapy in different cancers, we must consider how daily rhythms arise and synchronize in specific tissues. Given that about 80% of approved drugs in the United States hit targets known to rise and fall according to time of day and intrinsic

circadian rhythms,[104,105] it is possible that many therapeutics used to treat different cancers work best at specific times of day. It will be important to understand how circadian rhythms regulate tumor biology in a cell- and tissue-specific context. Altogether, this highly tractable and translatable approach can ultimately personalize patient care by determining when therapies should be given to cancer patients, depending on their individual circadian rhythms.

RESOURCE AVAILABILITY

Lead contact

Further information and requests for resources and reagents should be directed to and will be fulfilled by the lead contact, Dr. Erik D. Herzog (herzog@wustl.edu).

Materials availability

This study did not generate new unique reagents.

Data and code availability

- All data reported in this paper will be shared by the lead contact upon request.
- This paper does not report original code.
- Any additional information required to reanalyze the data reported in this paper is available from the lead contact upon request.

ACKNOWLEDGMENTS

The authors thank the members of the Herzog lab for valuable discussions and comments on the manuscript. This work was supported by National Institutes of Health grants NINDS R21NS120003, NCI R01NS134885, and the Washington University Siteman Cancer Center. Author M.F.G.-A. was supported by the Washington University Neuroscience Program T32-Training Grant NIH (T32NS121881-01) and the Initiative for Maximizing Student Development (IMSD) Program Training grant NIH (R25GM103757-10). Author A.R.D. was supported by the National Institutes of Health National Cancer Institute (F31CA250161).

AUTHOR CONTRIBUTIONS

All authors contributed to the study conception and design. Cell experiments and analysis: M.F.G.-A., A.R.D., T.S., and F.D. Animal experiments and analysis: M.F.G.-A., A.R.D., and N.A. ELISA and tissue processing: M.F.G.-A. and N.A. TCGA analysis: M.S.J., J.L., and J.B.R. The first draft of the manuscript was written by M.F.G.-A. and E.D.H. All authors read and approved the final manuscript.

DECLARATION OF INTERESTS

The authors declare no competing interests.

STAR★METHODS

Detailed methods are provided in the online version of this paper and include the following:

SUPPLEMENTAL INFORMATION

Supplemental information can be found online at https://doi.org/10.1016/j.ccell.2024.11.012.

Received: May 28, 2024
Revised: September 11, 2024
Accepted: November 19, 2024
Published: December 12, 2024

REFERENCES

1. Tamimi, A.F., and Juweid, M. (2017). Epidemiology and Outcome of Glioblastoma. In Glioblastoma, S. De Vleeschouwer, ed. (Codon Publications).
2. Cancer of the Brain and Other Nervous System - Cancer Stat Facts SEER. https://seer.cancer.gov/statfacts/html/brain.html,
3. Fernandes, C., Costa, A., Osório, L., Lago, R.C., Linhares, P., Carvalho, B., and Caeiro, C. (2017). Current Standards of Care in Glioblastoma Therapy. In Glioblastoma, S. De Vleeschouwer, ed. (Codon Publications).
4. Hottinger, A.F., Pacheco, P., and Stupp, R. (2016). Tumor treating fields: a novel treatment modality and its use in brain tumors. Neuro Oncol. *18*, 1338–1349. https://doi.org/10.1093/neuonc/now182.
5. Slat, E.A., Sponagel, J., Marpegan, L., Simon, T., Kfoury, N., Kim, A., Binz, A., Herzog, E.D., and Rubin, J.B. (2017). Cell-intrinsic, Bmal1-dependent Circadian Regulation of Temozolomide Sensitivity in Glioblastoma. J. Biol. Rhythm. *32*, 121–129. https://doi.org/10.1177/0748730417696788.
6. Damato, A.R., Luo, J., Katumba, R.G.N., Talcott, G.R., Rubin, J.B., Herzog, E.D., and Campian, J.L. (2021). Temozolomide chronotherapy in patients with glioblastoma: a retrospective single-institute study. Neurooncol. Adv. *3*, vdab041. https://doi.org/10.1093/noajnl/vdab041.
7. Damato, A.R., Katumba, R.G.N., Luo, J., Atluri, H., Talcott, G.R., Govindan, A., Slat, E.A., Weilbaecher, K.N., Tao, Y., Huang, J., et al. (2022). A randomized feasibility study evaluating temozolomide circadian medicine in patients with glioma. Neurooncol. Pract. *9*, 193–200. https://doi.org/10.1093/nop/npac003.
8. Gonzalez-Aponte, M.F., Damato, A.R., Trebucq, L.L., Simon, T., Cárdenas-García, S.P., Cho, K., Patti, G.J., Golombek, D.A., Chiesa, J.J., Rubin, J.B., and Herzog, E.D. (2024). Circadian regulation of MGMT expression and promoter methylation underlies daily rhythms in TMZ sensitivity in glioblastoma. J. Neuro Oncol. *166*, 419–430. https://doi.org/10.1007/s11060-023-04535-9.
9. Salvador, E., Shityakov, S., and Förster, C. (2014). Glucocorticoids and endothelial cell barrier function. Cell Tissue Res. *355*, 597–605. https://doi.org/10.1007/s00441-013-1762-z.
10. Kostaras, X., Cusano, F., Kline, G.A., Roa, W., and Easaw, J. (2014). Use of dexamethasone in patients with high-grade glioma: a clinical practice guideline. Curr. Oncol. *21*, e493–e503. https://doi.org/10.3747/co.21.1769.

11. Cenciarini, M., Valentino, M., Belia, S., Sforna, L., Rosa, P., Ronchetti, S., D'Adamo, M.C., and Pessia, M. (2019). Dexamethasone in Glioblastoma Multiforme Therapy: Mechanisms and Controversies. Front. Mol. Neurosci. *12*, 65. https://doi.org/10.3389/fnmol.2019.00065.

12. Hue, C.D., Cho, F.S., Cao, S., Dale" Bass, C.R., Meaney, D.F., and Morrison, B., 3rd (2015). Dexamethasone potentiates in vitro blood-brain barrier recovery after primary blast injury by glucocorticoid receptor-mediated upregulation of ZO-1 tight junction protein. J. Cerebr. Blood Flow Metabol. *35*, 1191–1198. https://doi.org/10.1038/jcbfm.2015.38.

13. Gu, Y.-T., Qin, L.-J., Qin, X., and Xu, F. (2009). The molecular mechanism of dexamethasone-mediated effect on the blood-brain tumor barrier permeability in a rat brain tumor model. Neurosci. Lett. *452*, 114–118. https://doi.org/10.1016/j.neulet.2008.12.047.

14. Gu, Y.t., Xue, Y.x., Wang, P., Zhang, H., Qin, L.j., and Liu, L.b. (2009). Dexamethasone enhances calcium-activated potassium channel expression in blood-brain tumor barrier in a rat brain tumor model. Brain Res. *1259*, 1–6. https://doi.org/10.1016/j.brainres.2008.12.080.

15. Kaup, B., Schindler, I., Knüpfer, H., Schlenzka, A., Preiss, R., and Knüpfer, M.M. (2001). Time-dependent inhibition of glioblastoma cell proliferation by dexamethasone. J. Neuro Oncol. *51*, 105–110. https://doi.org/10.1023/a:1010684921099.

16. Fan, Z., Sehm, T., Rauh, M., Buchfelder, M., Eyupoglu, I.Y., and Savaskan, N.E. (2014). Dexamethasone Alleviates Tumor-Associated Brain Damage and Angiogenesis. PLoS One *9*, e93264. https://doi.org/10.1371/journal.pone.0093264.

17. Piette, C., Deprez, M., Roger, T., Noël, A., Foidart, J.-M., and Munaut, C. (2009). The Dexamethasone-induced Inhibition of Proliferation, Migration, and Invasion in Glioma Cell Lines Is Antagonized by Macrophage Migration Inhibitory Factor (MIF) and Can Be Enhanced by Specific MIF Inhibitors. J. Biol. Chem. *284*, 32483–32492. https://doi.org/10.1074/jbc.M109.014589.

18. Liu, H., Huang, X., Wang, H., Shen, A., and Cheng, C. (2009). Dexamethasone inhibits proliferation and stimulates SSeCKS expression in C6 rat glioma cell line. Brain Res. *1265*, 1–12. https://doi.org/10.1016/j.brainres.2009.01.050.

19. Villeneuve, J., Galarneau, H., Beaudet, M.J., Tremblay, P., Chernomoretz, A., and Vallières, L. (2008). Reduced Glioma Growth Following Dexamethasone or Anti-Angiopoietin 2 Treatment. Brain Pathol. *18*, 401–414. https://doi.org/10.1111/j.1750-3639.2008.00139.x.

20. Gündisch, S., Boeckeler, E., Behrends, U., Amtmann, E., Ehrhardt, H., and Jeremias, I. (2012). Glucocorticoids Augment Survival and Proliferation of Tumor Cells. Anticancer Res. *32*, 4251–4261.

21. Luedi, M.M., Singh, S.K., Mosley, J.C., Hassan, I.S.A., Hatami, M., Gumin, J., Andereggen, L., Sulman, E.P., Lang, F.F., Stueber, F., et al. (2018). Dexamethasone-mediated oncogenicity in vitro and in an animal model of glioblastoma. J. Neurosurg. *129*, 1446–1455. https://doi.org/10.3171/2017.7.JNS17668.

22. Sur, P., Sribnick, E.A., Patel, S.J., Ray, S.K., and Banik, N.L. (2005). Dexamethasone decreases temozolomide-induced apoptosis in human gliobastoma T98G cells. Glia *50*, 160–167. https://doi.org/10.1002/glia.20168.

23. Das, A., Banik, N.L., Patel, S.J., and Ray, S.K. (2004). Dexamethasone protected human glioblastoma U87MG cells from temozolomide induced apoptosis by maintaining Bax:Bcl-2 ratio and preventing proteolytic activities. Mol. Cancer *3*, 36. https://doi.org/10.1186/1476-4598-3-36.

24. Langeveld, C.H., van Waas, M.P., Stoof, J.C., Sutanto, W., de Kloet, E.R., Wolbers, J.G., and Heimans, J.J. (1992). Implication of glucocorticoid receptors in the stimulation of human glioma cell proliferation by dexamethasone. J. Neurosci. Res. *31*, 524–531. https://doi.org/10.1002/jnr.490310316.

25. Kostopoulou, O.N., Mohammad, A.-A., Bartek, J., Winter, J., Jung, M., Stragliotto, G., Söderberg-Nauclér, C., and Landázuri, N. (2018). Glucocorticoids promote a glioma stem cell-like phenotype and resistance to chemotherapy in human glioblastoma primary cells: Biological and prognostic significance: Glucocorticoid-induced glioma stem cell phenotype. Int. J. Cancer *142*, 1266–1276. https://doi.org/10.1002/ijc.31132.

26. Moore, R.Y., and Eichler, V.B. (1972). Loss of a circadian adrenal corticosterone rhythm following suprachiasmatic lesions in the rat. Brain Res. *42*, 201–206. https://doi.org/10.1016/0006-8993(72)90054-6.

27. Oster, H., Damerow, S., Kiessling, S., Jakubcakova, V., Abraham, D., Tian, J., Hoffmann, M.W., and Eichele, G. (2006). The circadian rhythm of glucocorticoids is regulated by a gating mechanism residing in the adrenal cortical clock. Cell Metabol. *4*, 163–173. https://doi.org/10.1016/j.cmet.2006.07.002.

28. Oster, H., Challet, E., Ott, V., Arvat, E., de Kloet, E.R., Dijk, D.-J., Lightman, S., Vgontzas, A., and Van Cauter, E. (2017). The Functional and Clinical Significance of the 24-Hour Rhythm of Circulating Glucocorticoids. Endocr. Rev. *38*, 3–45. https://doi.org/10.1210/er.2015-1080.

29. Jones, J.R., Chaturvedi, S., Granados-Fuentes, D., and Herzog, E.D. (2021). Circadian neurons in the paraventricular nucleus entrain and sustain daily rhythms in glucocorticoids. Nat. Commun. *12*, 5763. https://doi.org/10.1038/s41467-021-25959-9.

30. Neumann, A.-M., Schmidt, C.X., Brockmann, R.M., and Oster, H. (2019). Circadian regulation of endocrine systems. Auton. Neurosci. *216*, 1–8. https://doi.org/10.1016/j.autneu.2018.10.001.

31. Lamia, K.A., Papp, S.J., Yu, R.T., Barish, G.D., Uhlenhaut, N.H., Jonker, J.W., Downes, M., and Evans, R.M. (2011). Cryptochromes mediate rhythmic repression of the glucocorticoid receptor. Nature *480*, 552–556. https://doi.org/10.1038/nature10700.

32. Dong, Z., Zhang, G., Qu, M., Gimple, R.C., Wu, Q., Qiu, Z., Prager, B.C., Wang, X., Kim, L.J.Y., Morton, A.R., et al. (2019). Targeting Glioblastoma Stem Cells through Disruption of the Circadian Clock. Cancer Discov. *9*, 1556–1573. https://doi.org/10.1158/2159-8290.CD-19-0215.

33. Trebucq, L.L., Cardama, G.A., Lorenzano Menna, P., Golombek, D.A., Chiesa, J.J., and Marpegan, L. (2021). Timing of Novel Drug 1A-116 to Circadian Rhythms Improves Therapeutic Effects against Glioblastoma. Pharmaceutics *13*, 1091. https://doi.org/10.3390/pharmaceutics13071091.

34. Damato, A.R., and Herzog, E.D. (2022). Circadian clock synchrony and chronotherapy opportunities in cancer treatment. Semin. Cell Dev. Biol. *126*, 27–36. https://doi.org/10.1016/j.semcdb.2021.07.017.

35. Kofuji, P., Mure, L.S., Massman, L.J., Purrier, N., Panda, S., and Engeland, W.C. (2016). Intrinsically Photosensitive Retinal Ganglion Cells (ipRGCs) Are Necessary for Light Entrainment of Peripheral Clocks. PLoS One *11*, e0168651. https://doi.org/10.1371/journal.pone.0168651.

36. Fukuhara, C., Inouye, S.I., Matsumoto, Y., Tsujimoto, G., Aoki, K., and Masuo, Y. (1998). Pituitary adenylate cyclase-activating polypeptide rhythm in the rat pineal gland. Neurosci. Lett. *241*, 115–118. https://doi.org/10.1016/s0304-3940(98)00041-x.

37. Holland, P.R., Barloese, M., and Fahrenkrug, J. (2018). PACAP in hypothalamic regulation of sleep and circadian rhythm: importance for headache. J. Headache Pain *19*, 20. https://doi.org/10.1186/s10194-018-0844-4.

38. Miller, J.-E.K., Granados-Fuentes, D., Wang, T., Marpegan, L., Holy, T.E., and Herzog, E.D. (2014). Vasoactive intestinal polypeptide mediates circadian rhythms in mammalian olfactory bulb and olfaction. J. Neurosci. *34*, 6040–6046. https://doi.org/10.1523/JNEUROSCI.4713-13.2014.

39. Aton, S.J., Colwell, C.S., Harmar, A.J., Waschek, J., and Herzog, E.D. (2005). Vasoactive intestinal polypeptide mediates circadian rhythmicity and synchrony in mammalian clock neurons. Nat. Neurosci. *8*, 476–483. https://doi.org/10.1038/nn1419.

40. Colwell, C.S., Michel, S., Itri, J., Rodriguez, W., Tam, J., Lelievre, V., Hu, Z., Liu, X., and Waschek, J.A. (2003). Disrupted circadian rhythms in VIP- and PHI-deficient mice. Am. J. Physiol. Regul. Integr. Comp. Physiol. *285*, R939–R949. https://doi.org/10.1152/ajpregu.00200.2003.

41. Refinetti, R. (2010). The circadian rhythm of body temperature. Front. Biosci. *15*, 564–594. https://doi.org/10.2741/3634.

42. Buhr, E.D., Yoo, S.-H., and Takahashi, J.S. (2010). Temperature as a universal resetting cue for mammalian circadian oscillators. Science *330*, 379–385. https://doi.org/10.1126/science.1195262.

43. Balsalobre, A., Brown, S.A., Marcacci, L., Tronche, F., Kellendonk, C., Reichardt, H.M., Schütz, G., and Schibler, U. (2000). Resetting of Circadian Time in Peripheral Tissues by Glucocorticoid Signaling. Science *289*, 2344–2347. https://doi.org/10.1126/science.289.5488.2344.

44. Cuesta, M., Cermakian, N., and Boivin, D.B. (2015). Glucocorticoids entrain molecular clock components in human peripheral cells. Faseb. J. *29*, 1360–1370. https://doi.org/10.1096/fj.14-265686.

45. Crosby, P., Hamnett, R., Putker, M., Hoyle, N.P., Reed, M., Karam, C.J., Maywood, E.S., Stangherlin, A., Chesham, J.E., Hayter, E.A., et al. (2019). Insulin/IGF-1 Drives PERIOD Synthesis to Entrain Circadian Rhythms with Feeding Time. Cell *177*, 896–909.e20. https://doi.org/10.1016/j.cell.2019.02.017.

46. Chi-Castañeda, D., and Ortega, A. (2018). Circadian Regulation of Glutamate Transporters. Front. Endocrinol. *9*, 340. https://doi.org/10.3389/fendo.2018.00340.

47. Damiola, F., Le Minh, N., Preitner, N., Kornmann, B., Fleury-Olela, F., and Schibler, U. (2000). Restricted feeding uncouples circadian oscillators in peripheral tissues from the central pacemaker in the suprachiasmatic nucleus. Genes Dev. *14*, 2950–2961. https://doi.org/10.1101/gad.183500.

48. Hirota, T., Lee, J.W., St John, P.C., Sawa, M., Iwaisako, K., Noguchi, T., Pongsawakul, P.Y., Sonntag, T., Welsh, D.K., Brenner, D.A., et al. (2012). Identification of small molecule activators of cryptochrome. Science *337*, 1094–1097. https://doi.org/10.1126/science.1223710.

49. Chun, S.K., Chung, S., Kim, H.-D., Lee, J.H., Jang, J., Kim, J., Kim, D., Son, G.H., Oh, Y.J., Suh, Y.-G., et al. (2015). A synthetic cryptochrome inhibitor induces anti-proliferative effects and increases chemosensitivity in human breast cancer cells. Biochem. Biophys. Res. Commun. *467*, 441–446. https://doi.org/10.1016/j.bbrc.2015.09.103.

50. Jang, J., Chung, S., Choi, Y., Lim, H.Y., Son, Y., Chun, S.K., Son, G.H., Kim, K., Suh, Y.-G., and Jung, J.-W. (2018). The cryptochrome inhibitor KS15 enhances E-box-mediated transcription by disrupting the feedback action of a circadian transcription-repressor complex. Life Sci. *200*, 49–55. https://doi.org/10.1016/j.lfs.2018.03.022.

51. Loh, D.H., Abad, C., Colwell, C.S., and Waschek, J.A. (2008). Vasoactive intestinal peptide is critical for circadian regulation of glucocorticoids. Neuroendocrinology *88*, 246–255. https://doi.org/10.1159/000140676.

52. Abe, M., Herzog, E.D., Yamazaki, S., Straume, M., Tei, H., Sakaki, Y., Menaker, M., and Block, G.D. (2002). Circadian rhythms in isolated brain regions. J. Neurosci. *22*, 350–356. https://doi.org/10.1523/JNEUROSCI.22-01-00350.2002.

53. Prolo, L.M., Takahashi, J.S., and Herzog, E.D. (2005). Circadian Rhythm Generation and Entrainment in Astrocytes. J. Neurosci. *25*, 404–408. https://doi.org/10.1523/JNEUROSCI.4133-04.2005.

54. Mure, L.S., Le, H.D., Benegiamo, G., Chang, M.W., Rios, L., Jillani, N., Ngotho, M., Kariuki, T., Dkhissi-Benyahya, O., Cooper, H.M., and Panda, S. (2018). Diurnal transcriptome atlas of a primate across major neural and peripheral tissues. Science *359*, eaao0318. https://doi.org/10.1126/science.aao0318.

55. Yoo, S.-H., Yamazaki, S., Lowrey, P.L., Shimomura, K., Ko, C.H., Buhr, E.D., Siepka, S.M., Hong, H.-K., Oh, W.J., Yoo, O.J., et al. (2004). PERIOD2::LUCIFERASE real-time reporting of circadian dynamics reveals persistent circadian oscillations in mouse peripheral tissues. Proc. Natl. Acad. Sci. USA *101*, 5339–5346. https://doi.org/10.1073/pnas.0308709101.

56. Yamamoto, T., Nakahata, Y., Soma, H., Akashi, M., Mamine, T., and Takumi, T. (2004). Transcriptional oscillation of canonical clock genes in mouse peripheral tissues. BMC Mol. Biol. *5*, 18. https://doi.org/10.1186/1471-2199-5-18.

57. Tosini, G., and Menaker, M. (1996). Circadian rhythms in cultured mammalian retina. Science *272*, 419–421. https://doi.org/10.1126/science.272.5260.419.

58. Zhang, R., Lahens, N.F., Ballance, H.I., Hughes, M.E., and Hogenesch, J.B. (2014). A circadian gene expression atlas in mammals: Implications for biology and medicine. Proc. Natl. Acad. Sci. USA *111*, 16219–16224. https://doi.org/10.1073/pnas.1408886111.

59. Yamazaki, S., Numano, R., Abe, M., Hida, A., Takahashi, R., Ueda, M., Block, G.D., Sakaki, Y., Menaker, M., and Tei, H. (2000). Resetting central and peripheral circadian oscillators in transgenic rats. Science *288*, 682–685. https://doi.org/10.1126/science.288.5466.682.

60. Kadmiel, M., and Cidlowski, J.A. (2013). Glucocorticoid receptor signaling in health and disease. Trends Pharmacol. Sci. *34*, 518–530. https://doi.org/10.1016/j.tips.2013.07.003.

61. Smith, L.K., and Cidlowski, J.A. (2010). Glucocorticoid-induced apoptosis of healthy and malignant lymphocytes. Prog. Brain Res. *182*, 1–30. https://doi.org/10.1016/S0079-6123(10)82001-1.

62. Distelhorst, C.W. (2002). Recent insights into the mechanism of glucocorticosteroid-induced apoptosis. Cell Death Differ. *9*, 6–19. https://doi.org/10.1038/sj.cdd.4400969.

63. Iglesias-Serret, D., de Frias, M., Santidrián, A.F., Coll-Mulet, L., Cosialls, A.M., Barragán, M., Domingo, A., Gil, J., and Pons, G. (2007). Regulation of the proapoptotic BH3-only protein BIM by glucocorticoids, survival signals and proteasome in chronic lymphocytic leukemia cells. Leukemia *21*, 281–287. https://doi.org/10.1038/sj.leu.2404483.

64. Schmidt, S., Rainer, J., Ploner, C., Presul, E., Riml, S., and Kofler, R. (2004). Glucocorticoid-induced apoptosis and glucocorticoid resistance: molecular mechanisms and clinical relevance. Cell Death Differ. *11*, S45–S55. https://doi.org/10.1038/sj.cdd.4401456.

65. Wang, Z., Malone, M.H., He, H., McColl, K.S., and Distelhorst, C.W. (2003). Microarray analysis uncovers the induction of the proapoptotic BH3-only protein Bim in multiple models of glucocorticoid-induced apoptosis. J. Biol. Chem. *278*, 23861–23867. https://doi.org/10.1074/jbc.M301843200.

66. Matthews, L.C., Berry, A.A., Morgan, D.J., Poolman, T.M., Bauer, K., Kramer, F., Spiller, D.G., Richardson, R.V., Chapman, K.E., Farrow, S.N., et al. (2015). Glucocorticoid receptor regulates accurate chromosome segregation and is associated with malignancy. Proc. Natl. Acad. Sci. USA *112*, 5479–5484. https://doi.org/10.1073/pnas.1411356112.

67. Aldaz, P., Auzmendi-Iriarte, J., Durántez, M., Lasheras-Otero, I., Carrasco-Garcia, E., Zelaya, M.V., Bragado, L., Olías-Arjona, A., Egaña, L., Samprón, N., et al. (2021). Identification of a Dexamethasone Mediated Radioprotection Mechanism Reveals New Therapeutic Vulnerabilities in Glioblastoma. Cancers *13*, 361. https://doi.org/10.3390/cancers13020361.

68. Pitter, K.L., Tamagno, I., Alikhanyan, K., Hosni-Ahmed, A., Pattwell, S.S., Donnola, S., Dai, C., Ozawa, T., Chang, M., Chan, T.A., et al. (2016). Corticosteroids compromise survival in glioblastoma. Brain *139*, 1458–1471. https://doi.org/10.1093/brain/aww046.

69. Dickmeis, T., Lahiri, K., Nica, G., Vallone, D., Santoriello, C., Neumann, C.J., Hammerschmidt, M., and Foulkes, N.S. (2007). Glucocorticoids Play a Key Role in Circadian Cell Cycle Rhythms. PLoS Biol. *5*, e78. https://doi.org/10.1371/journal.pbio.0050078.

70. O'Neill, J.S., and Reddy, A.B. (2012). The essential role of cAMP/Ca2+ signalling in mammalian circadian timekeeping. Biochem. Soc. Trans. *40*, 44–50. https://doi.org/10.1042/BST20110691.

71. Tischkau, S.A., Gallman, E.A., Buchanan, G.F., and Gillette, M.U. (2000). Differential cAMP gating of glutamatergic signaling regulates long-term state changes in the suprachiasmatic circadian clock. J. Neurosci. *20*, 7830–7837. https://doi.org/10.1523/JNEUROSCI.20-20-07830.2000.

72. Gillette, M.U., and Mitchell, J.W. (2002). Signaling in the suprachiasmatic nucleus: selectively responsive and integrative. Cell Tissue Res. *309*, 99–107. https://doi.org/10.1007/s00441-002-0576-1.

73. Bonsall, D.R., and Lall, G.S. (2013). Protein kinase C differentially regulates entrainment of the mammalian circadian clock. Chronobiol. Int. *30*, 460–469. https://doi.org/10.3109/07420528.2012.741170.

74. Jakubcakova, V., Oster, H., Tamanini, F., Cadenas, C., Leitges, M., van der Horst, G.T.J., and Eichele, G. (2007). Light entrainment of the mammalian circadian clock by a PRKCA-dependent posttranslational mechanism. Neuron *54*, 831–843. https://doi.org/10.1016/j.neuron.2007.04.031.

75. Schurov, I.L., Hepworth, T.J., and Hastings, M.H. (2002). Dopaminergic signalling in the rodent neonatal suprachiasmatic nucleus identifies a role for protein kinase A and mitogen-activated protein kinase in circadian entrainment. Eur. J. Neurosci. *15*, 223–232. https://doi.org/10.1046/j.0953-816x.2001.01848.x.

76. Sterniczuk, R., Yamakawa, G.R., Pomeroy, T., and Antle, M.C. (2014). Phase delays to light and gastrin-releasing peptide require the protein kinase A pathway. Neurosci. Lett. *559*, 24–29. https://doi.org/10.1016/j.neulet.2013.11.031.

77. Alessandro, M.S., Golombek, D.A., and Chiesa, J.J. (2019). Protein Kinases in the Photic Signaling of the Mammalian Circadian Clock. Yale J. Biol. Med. *92*, 241–250.

78. Pang, L., Dunterman, M., Xuan, W., Gonzalez, A., Lin, Y., Hsu, W.-H., Khan, F., Hagan, R.S., Muller, W.A., Heimberger, A.B., and Chen, P. (2023). Circadian regulator CLOCK promotes tumor angiogenesis in glioblastoma. Cell Rep. *42*, 112127. https://doi.org/10.1016/j.celrep.2023.112127.

79. Li, A., Lin, X., Tan, X., Yin, B., Han, W., Zhao, J., Yuan, J., Qiang, B., and Peng, X. (2013). Circadian gene Clock contributes to cell proliferation and migration of glioma and is directly regulated by tumor-suppressive miR-124. FEBS Lett. *587*, 2455–2460. https://doi.org/10.1016/j.febslet.2013.06.018.

80. Huang-Hobbs, E., Cheng, Y.-T., Ko, Y., Luna-Figueroa, E., Lozzi, B., Taylor, K.R., McDonald, M., He, P., Chen, H.-C., Yang, Y., et al. (2023). Remote neuronal activity drives glioma progression through SEMA4F. Nature *619*, 844–850. https://doi.org/10.1038/s41586-023-06267-2.

81. Venkatesh, H.S., Tam, L.T., Woo, P.J., Lennon, J., Nagaraja, S., Gillespie, S.M., Ni, J., Duveau, D.Y., Morris, P.J., Zhao, J.J., et al. (2017). Targeting neuronal activity-regulated neuroligin-3 dependency in high-grade glioma. Nature *549*, 533–537. https://doi.org/10.1038/nature24014.

82. Venkatesh, H.S., Morishita, W., Geraghty, A.C., Silverbush, D., Gillespie, S.M., Arzt, M., Tam, L.T., Espenel, C., Ponnuswami, A., Ni, L., et al. (2019). Electrical and synaptic integration of glioma into neural circuits. Nature *573*, 539–545. https://doi.org/10.1038/s41586-019-1563-y.

83. Pan, Y., Hysinger, J.D., Barron, T., Schindler, N.F., Cobb, O., Guo, X., Yalçın, B., Anastasaki, C., Mulinyawe, S.B., Ponnuswami, A., et al. (2021). NF1 mutation drives neuronal activity-dependent initiation of optic glioma. Nature *594*, 277–282. https://doi.org/10.1038/s41586-021-03580-6.

84. Anastasaki, C., Mo, J., Chen, J.-K., Chatterjee, J., Pan, Y., Scheaffer, S.M., Cobb, O., Monje, M., Le, L.Q., and Gutmann, D.H. (2022). Neuronal hyperexcitability drives central and peripheral nervous system tumor progression in models of neurofibromatosis-1. Nat. Commun. *13*, 2785. https://doi.org/10.1038/s41467-022-30466-6.

85. Krishna, S., Choudhury, A., Keough, M.B., Seo, K., Ni, L., Kakaizada, S., Lee, A., Aabedi, A., Popova, G., Lipkin, B., et al. (2023). Glioblastoma remodelling of human neural circuits decreases survival. Nature *617*, 599–607. https://doi.org/10.1038/s41586-023-06036-1.

86. Venkatesh, H.S., Johung, T.B., Caretti, V., Noll, A., Tang, Y., Nagaraja, S., Gibson, E.M., Mount, C.W., Polepalli, J., Mitra, S.S., et al. (2015). Neuronal Activity Promotes Glioma Growth through Neuroligin-3 Secretion. Cell *161*, 803–816. https://doi.org/10.1016/j.cell.2015.04.012.

87. Webb, A.B., Angelo, N., Huettner, J.E., and Herzog, E.D. (2009). Intrinsic, nondeterministic circadian rhythm generation in identified mammalian neurons. Proc. Natl. Acad. Sci. USA *106*, 16493–16498. https://doi.org/10.1073/pnas.0902768106.

88. Colwell, C.S. (2011). Linking neural activity and molecular oscillations in the SCN. Nat. Rev. Neurosci. *12*, 553–569. https://doi.org/10.1038/nrn3086.

89. Jones, J.R., Tackenberg, M.C., and McMahon, D.G. (2015). Manipulating circadian clock neuron firing rate resets molecular circadian rhythms and behavior. Nat. Neurosci. *18*, 373–375. https://doi.org/10.1038/nn.3937.

90. Mazuski, C., Abel, J.H., Chen, S.P., Hermanstyne, T.O., Jones, J.R., Simon, T., Doyle, F.J., and Herzog, E.D. (2018). Entrainment of Circadian Rhythms Depends on Firing Rates and Neuropeptide Release of VIP SCN Neurons. Neuron *99*, 555–563.e5. https://doi.org/10.1016/j.neuron.2018.06.029.

91. CIRCA: Circadian gene expression profiles. http://circadb.hogeneschlab.org/.

92. He, Y., Yi, W., Suino-Powell, K., Zhou, X.E., Tolbert, W.D., Tang, X., Yang, J., Yang, H., Shi, J., Hou, L., et al. (2014). Structures and mechanism for the design of highly potent glucocorticoids. Cell Res. *24*, 713–726. https://doi.org/10.1038/cr.2014.52.

93. Glass-Marmor, L., Paperna, T., Ben-Yosef, Y., and Miller, A. (2007). Chronotherapy using corticosteroids for multiple sclerosis relapses. J. Neurol. Neurosurg. Psychiatry *78*, 886–888. https://doi.org/10.1136/jnnp.2006.104000.

94. Cutolo, M. (2016). Glucocorticoids and chronotherapy in rheumatoid arthritis. RMD Open *2*, e000203. https://doi.org/10.1136/rmdopen-2015-000203.

95. Shapiro, W.R., Hiesiger, E.M., Cooney, G.A., Basler, G.A., Lipschutz, L.E., and Posner, J.B. (1990). Temporal effects of dexamethasone on blood-to-brain and blood-to-tumor transport of 14C-alpha-aminoisobutyric acid in rat C6 glioma. J. Neuro Oncol. *8*, 197–204. https://doi.org/10.1007/BF00177352.

96. Lévi, F., Okyar, A., Dulong, S., Innominato, P.F., and Clairambault, J. (2010). Circadian timing in cancer treatments. Annu. Rev. Pharmacol. Toxicol. *50*, 377–421. https://doi.org/10.1146/annurev.pharmtox.48.113006.094626.

97. Rivard, G.E., Infante-Rivard, C., Dresse, M.F., Leclerc, J.M., and Champagne, J. (1993). Circadian time-dependent response of childhood lymphoblastic leukemia to chemotherapy: a long-term follow-up study of survival. Chronobiol. Int. *10*, 201–204. https://doi.org/10.3109/07420529309073888.

98. Giacchetti, S., Bjarnason, G., Garufi, C., Genet, D., Iacobelli, S., Tampellini, M., Smaaland, R., Focan, C., Coudert, B., Humblet, Y., et al. (2006). Phase III Trial Comparing 4-Day Chronomodulated Therapy Versus 2-Day Conventional Delivery of Fluorouracil, Leucovorin, and Oxaliplatin As First-Line Chemotherapy of Metastatic Colorectal Cancer: The European Organisation for Research and Treatment of Cancer Chronotherapy Group. J. Clin. Orthod. *24*, 3562–3569. https://doi.org/10.1200/JCO.2006.06.1440.

99. Kobayashi, M., Wood, P.A., and Hrushesky, W.J.M. (2002). Circadian chemotherapy for gynecological and genitourinary cancers. Chronobiol. Int. *19*, 237–251. https://doi.org/10.1081/cbi-120002600.

100. Sephton, S.E., Sapolsky, R.M., Kraemer, H.C., and Spiegel, D. (2000). Diurnal cortisol rhythm as a predictor of breast cancer survival. J. Natl. Cancer Inst. *92*, 994–1000. https://doi.org/10.1093/jnci/92.12.994.

101. Kiessling, S., Beaulieu-Laroche, L., Blum, I.D., Landgraf, D., Welsh, D.K., Storch, K.-F., Labrecque, N., and Cermakian, N. (2017). Enhancing circadian clock function in cancer cells inhibits tumor growth. BMC Biol. *15*, 13. https://doi.org/10.1186/s12915-017-0349-7.

102. Iurisci, I., Filipski, E., Reinhardt, J., Bach, S., Gianella-Borradori, A., Iacobelli, S., Meijer, L., and Lévi, F. (2006). Improved tumor control through circadian clock induction by Seliciclib, a cyclin-dependent kinase inhibitor. Cancer Res. *66*, 10720–10728. https://doi.org/10.1158/0008-5472.CAN-06-2086.

103. Li, X.-M., Delaunay, F., Dulong, S., Claustrat, B., Zampera, S., Fujii, Y., Teboul, M., Beau, J., and Lévi, F. (2010). Cancer inhibition through circadian reprogramming of tumor transcriptome with meal timing. Cancer Res. *70*, 3351–3360. https://doi.org/10.1158/0008-5472.CAN-09-4235.

104. Adam, D. (2019). Core Concept: Emerging science of chronotherapy offers big opportunities to optimize drug delivery. Proc. Natl. Acad. Sci. USA *116*, 21957–21959. https://doi.org/10.1073/pnas.1916118116.

105. Sulli, G., Manoogian, E.N.C., Taub, P.R., and Panda, S. (2018). Training the circadian clock, clocking the drugs and drugging the clock to prevent, manage and treat chronic diseases. Trends Pharmacol. Sci. *39*, 812–827. https://doi.org/10.1016/j.tips.2018.07.003.

106. Sun, T., Warrington, N.M., Luo, J., Brooks, M.D., Dahiya, S., Snyder, S.C., Sengupta, R., and Rubin, J.B. (2014 Sep). Sexually dimorphic RB inactivation underlies mesenchymal glioblastoma prevalence in males. J Clin Invest *124* (9), 4123–4133. https://doi.org/10.1172/JCI71048.

107. Hastings, M.H., Reddy, A.B., McMahon, D.G., and Maywood, E.S. (2005). Analysis of circadian mechanisms in the suprachiasmatic nucleus by transgenesis and biolistic transfection. Methods Enzymol *393*, 579–592. https://doi.org/10.1016/S0076-6879(05)93030-9.

108. Liu, A.C., Tran, H.G., Zhang, E.E., Priest, A.A., Welsh, D.K., and Kay, S.A. (2008). Redundant function of REV-ERBalpha and beta and non-essential role for Bmal1 cycling in transcriptional regulation of intracellular circadian rhythms. PLoS Genet *4*, e1000023. https://doi.org/10.1371/journal.pgen.1000023.

109. Zhang, E.E., Liu, A.C., Hirota, T., Miraglia, L.J., Welch, G., Pongsawakul, P.Y., Liu, X., Atwood, A., Huss, J.W., 3rd, Janes, J., Su, A.I., Hogenesch, J.B., and Kay, S.A. (2009). A genome-wide RNAi screen for modifiers of the circadian clock in human cells. Cell *139*, 199–210. https://doi.org/10.1016/j.cell.2009.08.031.

110. Ramanathan, C., Khan, S.K., Kathale, N.D., Xu, H., and Liu, A.C. (2012). Monitoring cell-autonomous circadian clock rhythms of gene expression using luciferase bioluminescence reporters. J Vis Exp, 4234. https://doi.org/10.3791/4234.

Please cite this article in press as: Gonzalez-Aponte et al., Daily glucocorticoids promote glioblastoma growth and circadian synchrony to the host, Cancer Cell (2024), https://doi.org/10.1016/j.ccell.2024.11.012

STAR★METHODS

KEY RESOURCES TABLE

REAGENT or RESOURCE	SOURCE	IDENTIFIER
Antibodies		
Rabbit monoclonal anti-Glucocorticoid Receptor	Abcam	Cat# ab183127, RRID: AB_2833234
Rabbit polyclonal anti-Ki67	Abcam	Cat# ab15580, RRID: AB_443209
Donkey polyclonal anti-Rabbit IgG H&L (Alexa Fluor® 647)	Abcam	Cat# ab150075, RRID: AB_2752244
Bacterial and virus strains		
XL10-Gold Ultracompetent Cells	Agilent Technologies	Cat # 200315
Ef1α-luc	GenTarget Inc.	Cat# LVP434
Human NR3C1 shRNA lentivirus Target sequence: GTGTCACTGTTGGAGGTTATT	Sigma	Cat# SHCLNV, Clone ID TRCN0000245004
Human NR3C1 shRNA lentivirus Target sequence: CACAGGCTTCAGGTATCTTAT	Sigma	Cat# SHCLNV, Clone ID TRCN0000245005
Mouse NR3C1 shRNA lentivirus Target sequence: TGAGATTCGAATGACTTATAT	Sigma	Cat# SHCLNV, Clone ID TRCN0000238463
Mouse NR3C1 shRNA lentivirus Target sequence: TGGATAAGTCCATGAGTATTG	Sigma	Cat# SHCLNV, Clone ID TRCN0000238464
Human ARNTL shRNA lentivirus Target sequence: GCAGAATGTCATAGGCAAGTT	Sigma	Cat# SHCLNV, Clone ID TRCN0000019097
Human ARNTL shRNA lentivirus Target sequence: CTTCTAGGCACATCGTGTTAT	Sigma	Cat# SHCLNV, Clone ID TRCN0000331014
Biological samples		
Patient-derived xenograft B165	Dr. Albert Kim, Washington University in St. Louis	N/A
Chemicals, peptides, and recombinant proteins		
DAPI Solution (1 mg/mL)	Thermo Scientific	Cat# 62248
Corticosterone	Sigma	Cat# 27840
Hydrocortisone	Sigma	Cat# H0888
Dexamethasone	Sigma	Cat# D4902
Dexamethasone-Water Soluble	Sigma	Cat# D2915
D-Luciferin, Potassium Salt	GoldBio	Cat# LUC-10G
Polybrene	Sigma	Cat# TR-1003-G
Blasticidin	Thermo Fisher	Cat# AAJ67216XF
Puromycin	Thermo Fisher	Cat# ICN10055210
TRIzol reagent	Thermo Fisher	Cat# 15-596-026
Paraformaldehyde	Sigma	Cat# 441-244
Triton-X	VWR	Cat# EM-TX1568-1
ProLong Gold mounting medium with DAPI	Thermo Fisher	Cat# P36962
iTaqTM Universal SYBR® Green Supermix	Bio-Rad	Cat# #1725120
Gibco RPMI-1640 medium, no glutamine	Thermo Fisher	Cat# 21-870-076
Gibco DMEM/F12 medium, GlutaMAX supplemented	Thermo Fisher	Cat# 10-565-018
Fetal bovine serum, certified, heat-inactivated	Thermo Fisher	Cat# 10082-147
Gibco™ Penicillin-Streptomycin (10,000 U/mL)	Fisher Scientific	Cat# 15-140-122
Fugene 6	Fisher Scientific	Cat# PRE2691
L-Glutamine	Fisher Scientific	Cat# 25-030-081
B-27	Thermo Fisher	Cat# 17504-044
Heparin sodium salt from porcine	Sigma	Cat# H3149-25KU

(*Continued on next page*)

Please cite this article in press as: Gonzalez-Aponte et al., Daily glucocorticoids promote glioblastoma growth and circadian synchrony to the host, Cancer Cell (2024), https://doi.org/10.1016/j.ccell.2024.11.012

CellPress
OPEN ACCESS

Continued

REAGENT or RESOURCE	SOURCE	IDENTIFIER
Human FGF-basic (FGF-2/bFGF) (aa 1-155) Recombinant Protein	Thermo Fisher	Cat# PHG 0261
Gibco™ Human EGF Recombinant Protein	Fisher Scientific	Cat# PHG 0311
TrypLE™ Express Enzyme	Thermo Fisher	Cat# 12-605-010
Phosphate-buffered saline (PBS)	Sigma	Cat# 806-552
Albumin from bovine serum, 99% (BSA)	Sigma	Cat# A3059-50G
Ethanol	VWR	Cat# 71003-544
Methanol	Fisher Scientific	Cat# A456-500
Isoflurane solution	Covertus	Cat# 1169-5067-772
2,2,2-Thibromoethanol (Avertin)	Fisher Scientific	Cat# AC 42143
D-Sucrose	Fisher Scientific	Cat# BP 220-1
Tissue-Tek O.C.T	Electron Microscopy science	Cat# 62550-12
D- Glucose	Thermo Fisher	Cat# 150-23-021
KL001	Sigma	Cat# SML1032
KS15	MedChemExpress	Cat# HY-115672
Critical commercial assays		
Corticosterone ELISA Kit, strip wells	Cayman Chemical	Cat# 501320
Lenti-X™ GoStix™ Plus	Takara	Cat# 631280
Direct-zol RNA MiniPrep Plus kit	Zymo	Cat# R2071
SuperScript® III First-Strand Synthesis System	Thermo Fisher	Cat# 12574026
Deposited data		
Raw and analyzed data	This paper	–
Experimental models: Cell lines		
Hek293T/17 cells	ATCC	Cat# CRL-11268
GL261	Division of Cancer Treatment and Diagnosis Tumor Repository of the National Cancer Institute	N/A
NF1$^{-/-}$DNp53	Dr. Josh Rubin, Washington University in St. Louis	N/A
LN229	ATCC	Cat# CRL-2611
Experimental models: Organisms/strains		
C57BL/6NJ	Jackson Laboratory	Strain #005304 RRID:IMSR_JAX:005304
NCr-*Foxn1*^{nu} (nude mice)	Taconic	NCRNU RRID:IMSR_TAC:NCRNU
VIP KO	Dr. James Waschek, UCLA	N/A
Oligonucleotides		
Primer: mouse NR3C1 Forward Target sequence: CAA AGA TTG CAG GTA TCC TAT GAA	IDT	N/A
Primer: mouse NR3C1 Reverse Target sequence: TGG CTC TTC AGA CCT TCC TT	IDT	N/A
Primer: human NR3C1 Forward Target sequence: TATCCTCTGCCTCCCATTCT	IDT	N/A
Primer: human NR3C1 Reverse Target sequence: CACCTTCCTGTCTCCTGTTTAC	IDT	N/A
Primer: human Bmal1 Forward Target sequence: CCACGGTGGTGCTGGCTAGAG	IDT	N/A
Primer: human Bmal1 Reverse Target sequence: TCTTCCAAAAACCACAGTGCCCG	IDT	N/A

(*Continued on next page*)

Please cite this article in press as: Gonzalez-Aponte et al., Daily glucocorticoids promote glioblastoma growth and circadian synchrony to the host, Cancer Cell (2024), https://doi.org/10.1016/j.ccell.2024.11.012

Continued

REAGENT or RESOURCE	SOURCE	IDENTIFIER
Primer: mouse GAPDH Forward Target sequence: GGCAAATTCAACGGCACAGT	IDT	N/A
Primer: mouse GAPDH Reverse Target sequence: AGATGGTGATGGGCTTCCC	IDT	N/A
Primer: human GAPDH Forward Target sequence: ATGGGGAAGGTGAAGGTCG	IDT	N/A
Primer: human GAPDH Reverse Target sequence: GGGGTCATTGATGGCAACAATA	IDT	N/A
Recombinant DNA		
Bmal1-luc plasmid	Dr. Andrew Liu, University of Florida	N/A
Per2-luc plasmid	Dr. Andrew Liu, University of Florida	N/A
Packaging plasmid psPAX2	Addgene	Cat# 12260, RRID: Addgene_12260
Packaging plasmid pMD2.G	Addgene	Cat# 12259, RRID: Addgene_12259
Software and algorithms		
ImageJ		https://imagej.nih.gov/ij/
FIJI		https://imagej.net/software/fiji/
ChronoStar 1.0	Obtained from the Kramer Lab	https://www.achim-kramer-lab.de/downloads.html
Living Image Software	Perkin Elmer	https://resources.perkinelmer.com/corporate/content/lst_software_downloads/living_image_4.5_installation_licensing_guide.pdf
Lumicycle *in vivo*	Actimetrics	https://actimetrics.com/downloads/lumicycle/
ClockLab	Actimetrics	https://actimetrics.com/products/clocklab/
JTK cycle	Dr. Michael Hughes, Washington University in St. Louis	https://openwetware.org/wiki/File:JTKversion3.zip
GraphPad Prism (version 10.2.0)	GraphPad	https://www.graphpad.com/
Other		
Thermo Scientific Nunc EasYFlask 75cm2, treated	Thermo Fisher	Cat# 12-565-349
Corning Costar Cell Culture Plates 3516, 6-well	Fisher Scientific	Cat# 07-200-83
CELLTREAT Scientific Products PES Syringe Filter, 0.45m, 30mm, Sterile	Fisher Scientific	Cat# 50-202-064
100mm Falcon Bacteriological Petri Dishes with Lid	Thermo Fisher	Cat# 08-757-100D
Thermo Scientific Nunc EasYFlask 75cm2, treated	Thermo Fisher	Cat# 12-565-351
35mm BD Falcon petri dishes with lid	Fisher Scientific	Cat# 08-757-100A
Photon counting head (PMTs)	Hamamatsu Photonics	Cat# H9319-11

EXPERIMENTAL MODEL AND STUDY PARTICIPANT DETAILS

Glioblastoma cell culture

GL261

Glioma 261 (GL261, obtained from the Division of Cancer Treatment and Diagnosis Tumor Repository of the National Cancer Institute), a male murine model of GBM, were cultured in monolayer in coated T-75 flasks (Nunc Treated EasYFlasks, Fisher) using RPMI-1640 media (Sigma-Aldrich), supplemented with 10% FBS (Fisher), 1% L-Glutamine (Thermo Fisher), and 1% Pen/Strep (Thermo Fisher). Cells were grown in a 37°C incubator with a 5% CO2 environment. Passage number in all experiments ranged from four to eight.

$NF1^{-/-}$DNp53

$Nf1^{-/-}$DNp53 male astrocytes (generous gift of Dr. Josh Rubin), a murine model of GBM,[106] were cultured in monolayer in coated T-75 flasks (Nunc Treated EasYFlasks, Fisher) using 10mL DMEM/F12 media (Gibco), supplemented with 10% FBS (Fisher) and 1% Pen/

Strep (Thermo Fisher). Cells were grown in a 37°C incubator with a 5% CO2 environment. Passage number in all experiments ranged from four to eight.

B165

Human B165 (MGMT methylated, male), generous gift of Dr. Albert Kim, were cultured as spheres in 100mm uncoated petri dishes (Fisher) using 3mL DMEM/F12 Glutamax media (Gibco), supplemented with 1% Pen/Strep (Thermo Fisher), 2% B-27 (Miltenyi Biotec), 25ug/10mL Heparin (Sigma-Aldrich), 20ug/100ml EGF (Pepro Tech), and 2ug/100ml bFGF (Pepro Tech). Cells were grown in a 37°C incubator with a 5% CO2 environment. Passage number in all experiments ranged from six to ten.

LN229

LN229 (American Type Culture Collection), a female human cell line, were cultured in monolayer in coated T-75 flasks (Nunc Treated EasYFlasks, Fisher) using 10mL DMEM media (Gibco), supplemented with 5% FBS (Fisher), and 1% Pen/Strep (Thermo Fisher). Cells were grown in a 37°C incubator with a 5% CO2 environment. Passage number at implant ranged from four to eight.

Animals

C57BL/6NJ

10-week-old immunocompetent male and female C57BL/6NJ (The Jackson Laboratory, Strain #000664) mice were used in all experiments for orthotopic xenografting of murine GBM cells. Mice were singly housed in standard 12 h light/12 h dark conditions in individual wheel-cages to record locomotor activity in one-minute bins. After surgery, mice were monitored and treated with analgesic for three days. For some experiments, light schedules were shifted to a reversed 12h:12h dark/light, or to constant darkness (DD). At the end of all experiments, or when subjects lost 10% body weight from start to end of the experiment, mice were sacrificed in accordance with IACUC protocols and brain tissue was collected for subsequent analysis. Animal protocol number: #23-0105.

CrTac:Ncr-Foxn1nu10

10-week-old immunocompromised male and female CrTac:Ncr-Foxn1nu (Taconic, Strain #NCRNU) mice were used in all experiments for orthotopic xenografting of human and primary GBM cells. Mice were singly housed in standard 12 h light/12 h dark conditions in individual wheel-cages to record locomotor activity in one-minute bins. After surgery, mice were monitored and treated with analgesic for three days. For some experiments, light schedules were shifted to a reversed 12h:12h dark/light, or to constant darkness (DD). At the end of all experiments, or when subjects lost 10% body weight from start to end of the experiment, mice were sacrificed in accordance with IACUC protocols and brain tissue was collected for subsequent analysis.

VIP KO

10-week-old immunocompetent male and female VIP KO (obtained from: Dr. James Waschek, UCLA) mice were used in experiments for orthotopic xenografting of human and primary GBM cells. Mice were singly housed in constant darkness conditions in individual wheel-cages to record locomotor activity in one-minute bins. After surgery, mice were monitored and treated with analgesic for three days. At the end of all experiments, or when subjects lost 10% body weight from start to end of the experiment, mice were sacrificed in accordance with IACUC protocols and brain tissue was collected for subsequent analysis.

METHOD DETAILS

Experimental cell culture

GBM cells were grown to confluence (passage no. < 10) in supplemented media conditions mentioned in the "experimental model and study participant details" section, grown in a 37°C incubator with a 5% CO2 environment. Confluent cultures were kept for up to 4 weeks with media refreshed every 3-5 days. Once cultures reached 80% confluence, cells were split using TrypLE™ Express Enzyme (1X) (Gibco), centrifuged for 4 minutes at 0.4 RCF, diluted, and replated at a lower confluence in new cell culture flasks. Before the start of each experiment, cells were synchronized by changing culture media to a serum-free, supplemented with B27 (Thermo Fisher) "Air Media" (Bicarbonate-free, DMEM, 5mg/mL glucose, 0.35 mg/mL sodium bicarbonate, 0.01 M HEPES, 2 μg/mL pen/strep, 1% Glutamax, 1 mM luciferin, pH 7.4, 350 mOsm; adapted from Hastings et al., 2005),[107] and dishes were sealed with sterile vacuum grease.

Circadian luciferase lentivirus production

Lentiviral reporters expressing firefly luciferase driven by the mouse *Bmal1* (*Bmal1*-luc) (previously described in Liu et al., 2008;[108] Zhang et al., 2009)[109] or *Period2* (*Per2*-luc) (previously described in Ramanathan et al., 2012)[110] promoters were generated in the laboratory using plasmids (gift from Dr. Andrew Liu, University of Memphis) and packaging plasmids psPAX2 and pMD2.G (gift from Didier Trono (Addgene plasmid # 12260 and 12259; RRID:Addgene_12260 and 12259)). Hek293T/17 cells (ATCC) were plated at 3 million cells per 100 mm dish in complete DMEM media with 10% FBS (Thermo Fisher) and 5% Pen/Strep (Thermo Fisher) in a 5% CO_2 incubator for 24-30 hours. Before transfection, media was changed to DMEM with 5% FBS (Fisher) without any antibiotics. For transfection, cells were incubated with Fugene 6 (Promega) and plasmids for 12 hours, then changed to complete media. Viral particles in media were collected after 48 and 72 hours, centrifuged (RT, 3 min at 0.4 rcf) and filtered through a PES 0.45 um filter (Fisher). The presence of viral particles was confirmed with Lenti-X GoStix Plus test (Takara).

Please cite this article in press as: Gonzalez-Aponte et al., Daily glucocorticoids promote glioblastoma growth and circadian synchrony to the host, Cancer Cell (2024), https://doi.org/10.1016/j.ccell.2024.11.012

Lentiviral transductions

Luciferase reporters for Bmal1, Per2, & Ef1a

GBM cells were transduced with lentiviral reporters expressing firefly luciferase driven by the mouse *Bmal1* (*Bmal1*-luc), *Period2* (*Per2*-luc), or *Ef1α* (*Ef1α*-luc, obtained from GenTarget Inc.). Cells were grown in T-25cm^2 flasks for 24h and incubated for 10 minutes at 37°C in 3mL complete DMEM media with 10% FBS (Thermo Fisher), 5% Pen/Strep (Thermo Fisher), and 15μg polybrene (Millipore #TR-1003-G). Following incubation, 500uL of virus stock solution was added to each culture. Media was changed after 24 h at 37°C. Infected cells were selected using blasticidin (1.25 μg/mL, Thermo Fisher). Luciferase expression was confirmed by recording bioluminescence *in vitro*.

Glucocorticoid receptor knockdown

To knockdown *NR3C1* (GR) in LN229 and GL261 cells, two predesigned shRNA plasmids packaged into a lentivirus (vector pLKO.1) were obtained from Sigma Aldrich (Target sequences are listed in the key resources table). Cells were grown in T-25cm^2 flasks for 24h and incubated for 10 minutes at 37°C in 3mL complete DMEM media with 10% FBS (Thermo Fisher), 5% Pen/Strep (Thermo Fisher), and 15μg polybrene (Millipore #TR-1003-G). Following incubation, 10μL of virus stock solution was added to each culture. Media was changed after 24 h and cells were kept at 37°C, 5% CO2. Infected cells were selected using puromycin (1.5 μg/mL, Thermo Fisher) for 10 days. Knockdown efficiency was quantified by qPCR and immunocytochemistry. Two lentiviral constructs were independently tested.

Bmal1 knockdown

To knockdown *Bmal1* in LN229 cells, two predesigned shRNA plasmids packaged into a lentivirus (vector pLKO.1) were obtained from Sigma Aldrich (Target sequences are listed in the key resources table). Cells were grown in T-25cm^2 flasks for 24h and incubated for 10 minutes at 37°C in 3mL complete DMEM media with 10% FBS (Thermo Fisher), 5% Pen/Strep (Thermo Fisher), and 15μg polybrene (Millipore #TR-1003-G). Following incubation, 5-10μL of virus stock solution was added to each culture. Media was changed after 24 h and cells were kept at 37°C, 5% CO2. Infected cells were selected using puromycin (1.5 μg/mL, Thermo Fisher) for 10 days. Knockdown efficiency was quantified by qPCR and by recording *Per2*-luc bioluminescence *in vitro*. Two lentiviral constructs were independently tested.

Bioluminescence recordings *in vitro*

Cells were plated in 35 mm (BD Falcon, Fisher) petri dishes, synchronized by a media change, supplemented with 1mL of serum-free, B27 containing "Air DMEM media" containing 0.1mM D-luciferin (Goldbio), sealed with vacuum grease, and placed in a light-tight 36°C incubator containing photo-multiplier tubes (PMTs) (Hamamatsu Photonics). Each dish was placed under one PMT and bioluminescence was recorded as photons per 180 seconds.

Quantitative real-time PCR (qRT-PCR)

RNA was extracted from 500,000 cultured GBM cells using TRIzol reagent (Thermo Fisher). In some experiments, RNA was collected every 4 hours for a period of 48 hours. RNA was purified using the Direct-zol RNA MiniPrep Plus kit (Zymo) and cDNA was generated by RT-PCR using SuperScript® III First-Strand Synthesis System (Thermo Fisher). Gene expression changes were further probed using iTaqTM Universal SYBR® Green Supermix (Bio-Rad). The primer sequences for qRT-PCR are listed in the key resources table. PCR amplification was carried out at 40 cycles with 100ng of template DNA in triplicates. Protocol is as follows: Cycle 1: 95 °C for 3 min; Cycle 2: 95 °C for 30 s; Cycle 3: 60 °C for 30 s; repeat step 2–3 for 39 more times; Cycle 4: 72 °C for 1 min. Negative controls included no reverse transcriptase reactions and no template DNA samples. All procedures were done in triplicate in two biological replicates.

Immunocytochemistry

Cells were fixed using 4% PFA for 10 minutes, permeabilized for 30 min with 3% Triton-X (Millipore Sigma) in 1x PBS, and blocked for 1 hours with solution containing 10% BSA (Sigma) and 0.3% Triton-X. Primary antibodies were diluted in 2% blocking solution and incubated overnight at 4°C. Samples were then rinsed three times with 1x PBS and incubated in secondary antibody solution in 2% blocking solution for 1 hour at RT. Samples were rinsed 3 times in PBS, stained with ProLong Gold mounting medium with DAPI (Life Technologies, Carlsbad, CA), and stored in darkness at 4°C until imaging. Microscopy analysis was performed using ImageJ software. All antibodies and reagents used are listed in the key resources table.

In vitro glucocorticoid entrainment assays

To assess whether glucocorticoids shift *Per2* expression *in vitro*, GBM-P2L cells were plated as previously described for bioluminescence recordings *in vitro*. After at least 24h of recording, cells were acutely treated with 100nM Dexamethasone or vehicle (0.001% Ethanol), and bioluminescence was recorded for at least 2 days post-treatment. Bioluminescence data was detrended with a 24-hour moving average and analyzed in ChronoStar 1.0.

To assess if glucocorticoids entrain *Per2* expression, GBM-P2L cells were plated as previously described for bioluminescence recordings *in vitro*. After at least 24 hours of recording, cells were treated with 100μM Corticosterone or Cortisol, for murine or human cells, respectively, or vehicle (0.001% Ethanol). Glucocorticoids were given chronically for 3 days at the same time of day. Bioluminescence was continuously recorded for at least 2 days post-treatment. Bioluminescence data was detrended with a 24-hour moving average and analyzed in ChronoStar 1.0.

In vitro cell growth assays and pharmacology

We calculated total cell number by labeling cells with DAPI and measuring fluorescence at 405nm. Cells were seeded in 6-well plates at the same cell density (100,000 cells/well) and kept on an incubator for 48h to allow for cell growth. To assess intrinsic growth of GBM cells, individual cell culture plates were fixed with cold methanol and stained with 2μg/mL DAPI at either 24, 48, or 72h post-plating. To assess whether glucocorticoids promote GBM growth, cells were treated 48h post-plating with 100nM Dexamethasone (for human and murine cells), 100μM Cortisol (only for human cells), 100μM Corticosterone (only for murine cells), or vehicle (0.001% Ethanol for DEX cultures; water for Cortisol or Corticosterone). To assess whether glucocorticoids promote GBM growth at specific times of day and dependent on the circadian clock, cells were treated at two different time points with 100nM Dexamethasone in combination with either a Cryptochrome agonist (KL001, 1μM) or inhibitor (KS15, 1μM). In all experiments, cells were fixed 72h post-treatment with cold methanol and stained with 4′,6-diamidino-2-phenylindole (DAPI, 2 μg/mL). DAPI fluorescence was quantified with the Infinite 200 PRO plate reader (V_3.37_07/12_Infinite, Tecan Lifesciences).

Orthotopic xenografting

200,000 GBM cells were stereotactically implanted into the right caudate putamen (coordinates: Bregma, 2mm right laterally, 3mm ventral) of 10-week-old male and female NCr-Foxn1nu (Taconic Biosciences, Strain #NCRNU) for human models, C57BL/6NJ (The Jackson Laboratory, Strain #005304) for murine models, or VIP KO mice for murine models. After surgery, mice were housed in individual cages, monitored, and treated with analgesic for three days post-implant. Mice were allowed to recover and cells to engraft for 7 days before performing *in vivo* bioluminescence imaging to measure tumor size or daily rhythms in clock gene expression.

In vivo bioluminescence imaging

Mice were housed in standard 12 h light/12 h dark, reversed 12h dark/ 12 h light, or constant darkness (DD) conditions in wheel-cages to record locomotor activity in one-minute bins. Following orthotopic xenografting, tumor size was consistently measured at 1:00 p.m. by anesthetizing mice with 2% isoflurane, subcutaneously injecting them with 15 mg/mL of D-luciferin, allowing 10 min for it to access the brain, and imaging bioluminescence with 5 min exposure time. To measure daily clock gene expression in GBM xenografts, imaging was performed as described every 4h for 36h. All imaging was performed using an *In Vivo* Imaging System Lumina III (IVIS, Perkin Elmer). Bioluminescence images were analyzed using Living Image Software (Perkin Elmer).

For long-term recordings of daily clock gene expression, mice were individually placed in constant darkness in a light tight box containing two photomultiplier tubes (PMT, Hamamatsu H8259-01, Lumicycle *In Vivo*, Actimetrics). Mice received luciferin in their water (10 mM, Gold Biotechnology) *ad libitum* over the 2 days of recording. This method allowed for recording of *Per2* or *Bmal1* luciferase expression in freely moving mice. Animals were checked daily to ensure that they had adequate food and water.

Dexamethasone gavage *in vivo*

We prepared a fresh 25 mg/mL stock of water-soluble DEX (Sigma-Aldrich) each day approximately 10 min prior to the time of dosing (i.e., AM and PM). At the time of gavage, DEX was administered based on mouse weight to achieve a dose of 0.5 mg/kg. For gavage, mice were briefly anesthetized with 2% isoflurane and received between 100-200μL solution depending on mouse weight. DEX or vehicle was administered at either ZT4 (morning) or ZT12 (evening) for 6 consecutive days after tumor growth was established at 11 days post-implant. Total dose for mice receiving DEX equaled 3 mg/kg in all treatment groups. Treatment groups are as follows:

(1) DEX AM: Mice received 0.5 mg/kg DEX at ZT4 and vehicle at ZT12 for 6 consecutive days.
(2) DEX PM: Mice received vehicle at ZT4 and 0.5 mg/kg DEX at ZT12 for 6 consecutive days.
(3) Vehicle: Mice received vehicle at both ZT4 and ZT12 for 6 consecutive days.

Body weight measurements and survival

To assess tumor burden and disease progression, mice were weighed daily starting on the day of implant. At the end of the experiments, or when mice lost 10% of their body weight from 1st day of tumor implant, these were sacrificed in accordance with IACUC protocols. For tissue collection, Mice were anesthetized with intraperitoneal Avertin (tribromoethanol), then transcardially perfused with 10mL of PBS followed by 10mL of 4% paraformaldehyde (PFA).

Locomotor activity recording

Mice were singly housed in standard 12 h light/12 h dark, reversed 12h dark/ 12 h light, or constant darkness (DD) conditions in wheel-cages to record locomotor activity in one-minute bins. Wheel-running activity was continuously recorded for 2 weeks before tumor implant to allow for mouse habituation to new cages and single housing, and throughout the end of each experiment.

Fecal corticosterone analysis

Mice were placed in custom-built collectors, maintained in a temperature-, humidity-, and light-controlled chamber with food and water provided *ad libitum* to allow for non-invasive measurement of fecal corticosterone from individual mice, a validated method for measuring circadian rhythms in corticosterone release. Mice were allowed to habituate in the cages for at least 7 days before beginning fecal pellet collection. Fecal pellets were collected every hour for a total of 28h. We next removed the collected fecal pellets

from the dish, placed them into individual tubes, and baked them at 62°C until completely dry, typically 2–3 days. Timepoints were binned into 4-hour groups for further processing, and the resultant samples were grounded into a fine powder using a mortar and pestle. We weighed out 20 mg of each sample, added 1 mL of 80% methanol, and agitated for 40 min to extract steroids. After centrifuging, supernatant was transferred to new tubes and placed in a fume hood until methanol fully evaporated (~7 days). Dried samples were resuspended in 200 μL enzyme-linked immunosorbent assay (ELISA) buffer (Cayman Chemical, Ann Arbor, MI) and then diluted 1:50 in ELISA buffer. We processed the samples in triplicate for corticosterone concentration using the instructions in the ELISA kit (Corticosterone ELISA Kit, Cayman Chemical). Absorbance values were measured using a microplate reader at 415 nm (iMark; BioRad, Hercules, CA) and final corticosterone concentrations (in pg/mL) were determined based on the standard curve and dilution factor.

Immunohistochemistry

Brains were collected and fixed in 4% PFA overnight at 4°C, then transferred to a sucrose gradient for cryoprotection. Brains were embedded in Tissue-Tek O.C.T. and sectioned in the coronal plane at 40μm using a sliding microtome. Slices were then permeabilized for 30 min with 3% Triton-X in 1x PBS, and blocked for 1 hour with solution containing 10% BSA and 0.3% Triton-X. Primary antibodies were diluted in 2% blocking solution and incubated overnight at 4°C. Sections were then rinsed three times with 1x PBS and incubated in secondary antibody solution in 2% blocking solution for 2 hours at RT. Sections were rinsed 3 times in PBS, mounted with ProLong Gold mounting medium with DAPI (Life Technologies, Carlsbad, CA), and stored in darkness at 4°C until imaging. Microscopy analysis was performed using ImageJ software. All antibodies and reagents used are listed in the key resources table.

Analysis of NR3C1 mRNA gene expression in The Cancer Genome Atlas (TCGA) GBM

We accessed the TCGA GBM cohort for mRNA gene expression data (on the microarray platform HG-UG133A) and patient clinical and survival data from the Gliovis data portal (http://gliovis.bioinfo.cnio.es/). IDH mutant GBM tumors were excluded from all analyses. The NR3C1 mRNA gene expression level was extracted. A violin plot was generated to visualize NR3C1 expression level between GBM tumors (N=498) and non-tumor normal samples (N=10) and Wilcoxon rank sum test was applied to compare the expression difference. To further investigate the impact of NR3C1 on patient survival accounting for covariates in the GBM patients (N=271 after omitting cases with missing data in MGMT methylation), we fit a Cox proportional hazard model on patients' overall survival with NR3C1 (in continuous logarithm scale), with incorporation of known risk factors available in the TCGA GBM cohort, including age (continuous scale), sex (male vs. female), subtype (classical, proneural, mesenchymal), and MGMT (O6-methylguanine-DNA methyltransferase) promoter methylation status (unmethylated vs. methylated). Graphical examination of the scaled Schoenfeld residuals support the proportionality assumption of the Cox model.

QUANTIFICATION AND STATISTICAL ANALYSIS

Circadian analyses

The correlation coefficient (CC) of a best-fit circadian cosine function was calculated using ChronoStar 1.0 to assess circadian rhythmicity in GBM cells. CC values above 0.7 were circadian and are reported in figure legends and text. For *in vivo* bioluminescence data, JTK cycle was used to assess circadian rhythmicity, and p value is reported in figure legends and text. A level of $p < 0.05$ was used to designate circadian rhythmicity.

Statistics

Data are presented as mean±SEM. To calculate synchronization index (SI) based on Raleigh circular statistics, we used the time of daily peak *Per2* expression from the GBM xenograft of each individual mouse. A SI of 1.0 indicates that *Per2* expression in GBM xenografts peaked at the same time of day across all mice and a SI of 0.0 indicates they peaked at random times. Statistical significance of mean differences was determined by either i) Student's t tests; ii) one-way analysis of variance (one-way ANOVA) with multiple comparisons test; or iii) two-way analysis of variance (two-way ANOVA) with multiple comparisons test. The sample size (n), statistical analysis, and multiple comparisons test used is reported within the figures or legends for each experiment. A level of $p < 0.05$ was used to designate significant differences. P-values are reported using the following symbolic representation: ns = $p > 0.05$, * = $p \leq 0.05$, ** = $p \leq 0.01$, *** = $p \leq 0.001$, **** = $p \leq 0.0001$. All the statistical analyses were performed using GraphPad Prism (version 10.3.1).